

This is a preprint of an article accepted for publication in Journal of Engineering Structures on 12 April 2010. The published article is available online at <http://www.sciencedirect.com/science/article/pii/S0141029610001483>. To be cited as: Miquel B., Bouaanani N. 2010. Simplified evaluation of the vibration period and seismic response of gravity dam-water systems. Journal of Engineering Structures, 32: 2488-2502.

Simplified evaluation of the vibration period and seismic response of gravity dam-water systems

Benjamin Miquel¹ and Najib Bouaanani²

ABSTRACT

This paper proposes a practical procedure for a simplified evaluation of the fundamental vibration period of dam-water systems, and corresponding added damping, force and mass, all key parameters to assess the seismic behavior. The proposed technique includes the effects of dam geometry and flexibility, dam-reservoir interaction, water compressibility and varying reservoir level. The mathematical derivations of the method are provided considering both incompressible and compressible water assumptions. In the former case, we propose a closed-form expression for the fundamental vibration period of a dam-reservoir system. When water compressibility is included, we show that the fundamental vibration period can be obtained by simply solving a cubic equation. The proposed procedure is validated against classical Westergaard added mass formulation as well as other more advanced analytical and finite element techniques. Gravity dam monoliths with various geometries and rigidities impounding reservoirs with different heights are investigated. The new approach yields results in excellent agreement with those obtained when the reservoir is modeled analytically, or numerically using potential-based finite elements. The analytical expressions developed and the procedure steps are presented in a manner so that calculations can be easily implemented in a spreadsheet or program for simplified and practical seismic analysis of gravity dams.

KEY WORDS: Gravity dams; Dam-reservoir systems; Fluid-structure interaction; Analytical formulations; Finite elements; Dam safety; Vibration period; Earthquake response; Simplified methods.

¹ Graduate Research Assistant, Department of Civil, Geological and Mining Engineering, École Polytechnique de Montréal, Montréal, QC H3C 3A7, Canada.

² Associate Professor, Department of Civil, Geological and Mining Engineering, École Polytechnique de Montréal, Montréal, QC H3C 3A7, Canada
Corresponding author. E-mail: najib.bouaanani@polymtl.ca

Nomenclature

Abbreviations

ESDOF Equivalent single degree of freedom

FRF Frequency response function

Roman symbols

A_1, A_2, A_3, A_4 coefficients given by Eqs. (59) to (63)

a_1, a_2, a_3 coefficients used for cubic approximation of structural mode shapes

B_0, B_1 hydrodynamic parameters given by Eqs. (22) and (23), respectively

B_{0n}, B_{1n} hydrodynamic parameters given by Eqs. (24) and (25), respectively

$\hat{B}_{0n}, \hat{B}_{1n}$ hydrodynamic parameters given by Eqs. (32) and (33), respectively

C_n, \tilde{C}_n n^{th} generalized damping of the dam and dam-reservoir system, respectively

C_r velocity of pressure waves in the reservoir

D_1, D_2 coefficients given by Eq. (65)

E_s modulus of elasticity of the dam

F_{st} total hydrostatic force exerted on dam upstream face

F_n, G_n functions given by Eq. (34)

f_1 equivalent lateral force given by Eq. (80)

f_{sc} equivalent lateral force including higher mode effects as given by Eq. (83)

H_r, H_s reservoir and dam heights, respectively

I_{jn} integral given by Eq. (8)

K_1 generalized stiffness of the dam at fundamental vibration mode

L_n, \tilde{L}_n n^{th} generalized forces of the dam and dam-reservoir system, respectively

M mass matrix of the dam monolith

M_s total mass of the dam monolith

m_i	Westergaard added mass at node i of the dam finite element mesh
M_n, \widetilde{M}_n	n^{th} generalized masses of the dam and dam-reservoir system, respectively
N_r, N_s	number of considered reservoir and structural modes, respectively
$\bar{\mathbf{Q}}, \bar{Q}_n$	vector in Eq. (11) and its elements given by Eq. (13), respectively
p, \bar{p}	hydrodynamic pressure and corresponding FRF, respectively
\bar{p}_0, \bar{p}_j	hydrodynamic pressure FRFs given by Eq. (3)
$\bar{p}_{0n}, \bar{p}_{jn}$	hydrodynamic pressure FRFs given by Eqs. (4) and (5), respectively
$\widehat{\bar{p}}_0$	real-valued hydrodynamic pressure given by Eq. (84)
R_1, R_r	frequency ratios given by ω_1/ω_0 and ω_r/ω_0 , respectively
$\bar{\mathbf{S}}, \bar{S}_{nj}$	matrix in Eq. (11) and its elements given by Eq. (12), respectively
S_a	pseudo-acceleration ordinate of the earthquake design spectrum
t	time
T_1, T_r	fundamental periods of the dam and dam-reservoir system, respectively
U	coefficient given by Eq. (67)
$\bar{u}, \bar{\ddot{u}}$	FRFs for horizontal displacement and acceleration, respectively
V	coefficient given by Eq. (67)
V_i	volume of water tributary to node i of the dam finite element mesh
$\bar{v}, \bar{\ddot{v}}$	FRFs for vertical displacement and acceleration, respectively
$\ddot{x}_g, \ddot{x}_g^{(\text{max})}$	ground acceleration time history and peak ground acceleration, respectively
y_i	height of node i of the dam finite element mesh
$\bar{\mathbf{Z}}, \bar{Z}_j$	vector of generalized coordinates and j^{th} generalized coordinate, respectively
<i>Greek symbols</i>	
$\gamma_i, \widehat{\gamma}_i$	coefficients given in Table 1 for $i = 1 \dots 6$
Γ	variable given by Eq. (65)

$\Gamma_1, \Gamma_2, \Gamma_3, \Gamma_4$	analytical solutions of Eq. (64) as given by Eq. (66)
Γ^*	real solution of Eq. (64)
Δ	discriminant of Eq. (64)
δ_{nj}	Kronecker symbol
ε	error estimator
$\zeta_i, \hat{\zeta}_i$	coefficients given in Table 2 for $i = 1 \dots 3$
η	ratio of reservoir level to dam height, i.e. H_r/H_s
$\theta, \hat{\theta}, \Theta$	parameters given by Eqs. (76), (43) and (42), respectively
κ_n	function given by Eq. (7)
λ_n	n^{th} reservoir eigenvalue
μ_s	mass of the dam per unit height
ν	Poisson's ratio of dam concrete
ξ_n	n^{th} fraction of critical damping of the dam
$\tilde{\xi}_r$	equivalent damping ratio of the dam-reservoir ESDOF system
ρ_r, ρ_s	mass densities of water and dam concrete, respectively
τ	coefficient given by Eq. (67)
$\varphi, \hat{\varphi}, \Phi$	parameters given by Eqs. (57), (39) and (38), respectively
χ	frequency parameter defined by R_r^2
$\psi_n, \psi_j^{(x)}$	n^{th} structural mode shape and x -component of the j^{th} structural mode shape
ω	exciting frequency
ω_0	fundamental vibration frequency of the full reservoir
ω_n	n^{th} vibration frequency of the dam
ω_r	fundamental vibration frequency of the dam-reservoir system

1 Introduction

Considering the effects of fluid-structure dynamic interactions is important for the design and safety evaluation of earthquake-excited gravity dams. Significant research has been devoted to this subject since the pioneering work of Westergaard [1] who modeled hydrodynamic loads as an added-mass attached to the dam upstream face. Although Westergaard's analytical formulation was developed assuming a rigid dam impounding incompressible water, it has been widely used for many decades to design earthquake-resistant concrete dams because of its simplicity. During the last four decades, several researchers developed advanced analytical and numerical approaches to account for dam deformability and water compressibility in the seismic response of concrete dams [2–12]. Most of these methods are based on a coupled field solution through sub-structuring of the dam-reservoir system, making use of analytical formulations, finite elements, boundary elements or a mix of these techniques. In the approach proposed by Chopra and collaborators [2–4, 7], the reservoir is modeled analytically as a continuum fluid region extending towards infinity in the upstream direction. When finite or boundary elements are used, the reservoir has to be truncated at a finite distance and appropriate transmitting boundary conditions have to be applied at the cutting boundaries to prevent reflection of spurious waves as discussed by the authors in a previous work [13]. Some procedures were implemented in numerical codes specialized in two- and three-dimensional analyses of concrete dams [9, 14], and some were validated against experimental findings from in-situ forced-vibration tests [15–18]. Although such sophisticated techniques were proven to efficiently handle many aspects of dam-reservoir interactions, their use requires appropriate expertise and specialized software. For practical engineering applications, simplified procedures are still needed to globally evaluate the seismic response of gravity dams, namely for preliminary design or safety evaluation purposes [19–21].

The fundamental vibration period of dam-reservoir systems is a key factor in the assessment of their dynamic or seismic behavior. Most seismic provisions and simplified procedures use the fundamental vibration period as an input parameter to determine seismic design accelerations and forces from a site-specific earthquake response spectrum. It is therefore crucial to dispose of accurate and yet practical expressions to evaluate the fundamental period of gravity dams dynamically interacting with their impounded reservoirs. Hatanaka [22] developed simplified expressions to estimate the fundamental vibration period of dams with empty reservoirs. He approximated the dam geometry as a symmetrical triangle and distinguished the cases where bending or shear effects are predominant in the dynamic response of the dam. Considering analogy with beam theory, Okamoto [23] proposed simplified formulas to estimate the fundamental vibration periods of dams with empty and full reservoirs. Chopra [2, 4] analyzed several idealized triangular dam cross-sections to obtain an approximate fundamental vibration period and corresponding mode shape of typical gravity dams with an empty reservoir. These standard dynamic properties and related quantities were implemented in simplified earthquake response analyses of gravity dams [19, 20]. To determine the fundamental vibration period of a dam including impounded water effects, Chopra and collaborators [2–4, 7, 15] first obtained the frequency response curves char-

acterizing dam-reservoir vibrations, and then identified the fundamental vibration frequency as the one corresponding to the first resonance on the curves. The authors found that hydrodynamic effects lengthen the fundamental vibration period of gravity dams and the results obtained for standard dam cross-sections were presented in figures and tables [19].

As mentioned above, although significant work has been devoted to investigate the effects of dam-water interaction on the dynamic response of gravity dams, there is no available practical closed-form technique to accurately estimate the fundamental vibration period of a gravity dam including hydrodynamic effects. In this work, we propose simplified analytical expressions and a systematic procedure to rigorously determine the fundamental period of vibrating dam-reservoir systems and corresponding added damping, force and mass. The method includes the effects of dam geometry and flexibility, water compressibility and varying reservoir level. Formulations assuming either incompressible or compressible impounded water are developed. To assess the efficiency and accuracy of the proposed procedure, we validate it against classical Westergaard added mass formulation as well as other advanced analytical and finite element techniques. We finally illustrate how the proposed technique can be efficiently implemented in a simplified and practical earthquake analysis of dam-reservoir systems.

2 Analytical formulation for vibrating dam-reservoir systems

2.1 Basic assumptions

The formulation described in this section was originally developed by Fenves and Chopra [7] to investigate earthquake excited gravity dams impounding semi-infinite rectangular-shape reservoirs. The approach is based on a sub-structuring technique, where the dam is modeled using finite elements and reservoir effects are accounted for analytically through hydrodynamic loads applied at dam upstream face. The hydrodynamic pressures are obtained by first determining mode shapes of the dam with an empty reservoir and then applying these mode shapes as boundary conditions to the solution of Helmholtz equation that governs reservoir motion in the frequency domain. Bouaanani and Lu [24] showed that this procedure to include dam-reservoir interaction yields excellent results when compared to techniques where the reservoir is modeled numerically using potential-based fluid finite elements. The basic equations of the formulation are reviewed in this section considering compressible and incompressible water assumptions.

To illustrate the dynamics of dam-reservoir systems, we consider a 2D gravity dam cross-section shown in Fig. 1. The dam has a total height H_s and it impounds a semi-infinite reservoir of constant depth H_r . A Cartesian coordinate system with axes x and y with origin at the heel of the structure is adopted and the following main assumptions are made : (i) the dam and water are assumed to have a linear elastic behavior; (ii) the dam foundation is assumed rigid; (iii) the water in the reservoir is assumed inviscid, with its motion irrotational and limited to small amplitudes; and (iv) gravity surface waves are neglected.

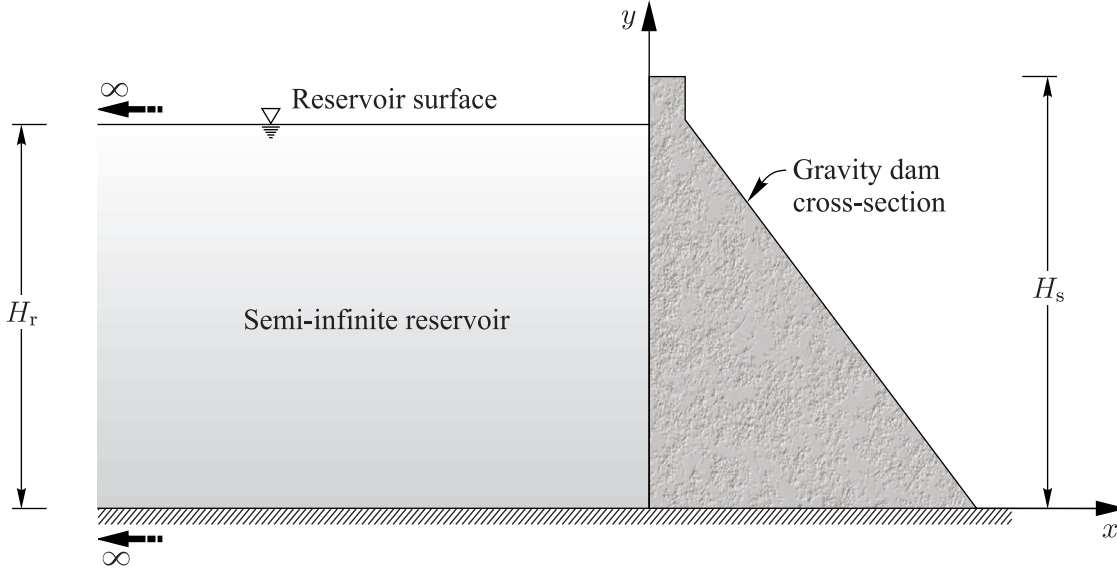


Figure 1. Dam-reservoir system.

2.2 Coupling hydrodynamic pressure and dam structural response

Considering a unit horizontal and harmonic exciting free-field ground motion $\ddot{x}_g(t) = e^{i\omega t}$, the hydrodynamic pressure in the reservoir can be expressed in the frequency domain as $p(x, y, t) = \bar{p}(x, y, \omega) e^{i\omega t}$, where ω denotes the exciting frequency, and $\bar{p}(x, y, \omega)$ a complex-valued frequency response function (FRF) obeying the classical Helmholtz equation

$$\frac{\partial^2 \bar{p}}{\partial x^2} + \frac{\partial^2 \bar{p}}{\partial y^2} + \frac{\omega^2}{C_r^2} \bar{p} = 0 \quad (1)$$

where C_r is the velocity of pressure waves in water. Fenves and Chopra [7] showed that hydrodynamic pressure FRF \bar{p} can be decomposed as

$$\bar{p}(x, y, \omega) = \bar{p}_0(x, y, \omega) - \omega^2 \sum_{j=1}^{N_s} \bar{Z}_j(\omega) \bar{p}_j(x, y, \omega) \quad (2)$$

in which \bar{p}_0 is the FRF for hydrodynamic pressure at rigid dam upstream face due to ground acceleration, \bar{p}_j the FRF for hydrodynamic pressure due to horizontal acceleration $\psi_j^{(x)}(0, y)$ of the dam upstream face where $\psi_j^{(x)}$ is the x -components of the j^{th} structural mode shape ψ_j , \bar{Z}_j the corresponding generalized coordinate and N_s the total number of mode shapes included in the analysis.

The complex FRFs \bar{p}_0 and \bar{p}_j can be expressed as the summation of N_r FRFs \bar{p}_{0n} and \bar{p}_{jn} corresponding

each to a reservoir mode n

$$\bar{p}_0(x, y, \omega) = \sum_{n=1}^{N_r} \bar{p}_{0n}(x, y, \omega); \quad \bar{p}_j(x, y, \omega) = \sum_{n=1}^{N_r} \bar{p}_{jn}(x, y, \omega) \quad (3)$$

FRFs \bar{p}_{0n} and \bar{p}_{jn} are given by

$$\bar{p}_{0n}(x, y, \omega) = \frac{4\rho_r}{\pi} \frac{(-1)^n}{(2n-1)} \frac{e^{\kappa_n(\omega)x}}{\kappa_n(\omega)} \cos(\lambda_n y) \quad (4)$$

$$\bar{p}_{jn}(x, y, \omega) = -2\rho_r I_{jn} \frac{e^{\kappa_n(\omega)x}}{\kappa_n(\omega)} \cos(\lambda_n y) \quad (5)$$

where ρ_r denotes water mass density and where the frequency-independent eigenvalues λ_n and terms κ_n and I_{jn} are given by

$$\lambda_n = \frac{(2n-1)\pi}{2H_r} \quad (6)$$

$$\kappa_n(\omega) = \sqrt{\lambda_n^2(\omega) - \frac{\omega^2}{C_r^2}} \quad (7)$$

$$I_{jn} = \frac{1}{H_r} \int_0^{H_r} \psi_j^{(x)}(0, y) \cos(\lambda_n y) dy \quad (8)$$

When water compressibility is neglected, i.e. $C_r \rightarrow +\infty$, Eq. (7) yields the frequency-independent term $\kappa_n = \lambda_n$. Eqs. (4) and (5) simplify then to

$$\bar{p}_{0n}(x, y) = \frac{8\rho_r H_r}{\pi^2} \frac{(-1)^n}{(2n-1)^2} e^{\lambda_n x} \cos(\lambda_n y) \quad (9)$$

$$\bar{p}_{jn}(x, y) = -\frac{4\rho_r H_r}{\pi} \frac{I_{jn}}{(2n-1)} e^{\lambda_n x} \cos(\lambda_n y) \quad (10)$$

Using modal superposition and mode shapes orthogonality, we show that the vector $\bar{\mathbf{Z}}$ of frequency-dependent generalized coordinates \bar{Z}_j , $j = 1 \dots N_s$, can be obtained by solving the system of equations

$$\bar{\mathbf{S}} \bar{\mathbf{Z}} = \bar{\mathbf{Q}} \quad (11)$$

in which, for $n = 1 \dots N_s$ and $j = 1 \dots N_s$

$$\bar{S}_{nj}(\omega) = \left(\omega_n^2 - \omega^2 + 2i\omega \omega_n \xi_n \right) M_n \delta_{nj} + \omega^2 \int_0^{H_r} \bar{p}_j(0, y, \omega) \psi_n^{(x)}(0, y) dy \quad (12)$$

$$\bar{Q}_n(\omega) = -L_n + \int_0^{H_r} \bar{p}_0(0, y, \omega) \psi_n^{(x)}(0, y) dy \quad (13)$$

with

$$M_n = \boldsymbol{\psi}_n^T \mathbf{M} \boldsymbol{\psi}_n; \quad L_n = \boldsymbol{\psi}_n^T \mathbf{M} \mathbf{1} \quad (14)$$

and where δ_{nj} is the Kronecker symbol, $\mathbf{1}$ is a column vector with ones when a horizontal translational degree of freedom corresponds to the direction of earthquake excitation, and zero otherwise, \mathbf{M} is the dam mass matrix, ω_n is the vibration frequency along mode shape ψ_n , and ξ_n , M_n and L_n are the corresponding modal damping ratio, generalized mass and force, respectively. When mode shapes are also mass-normalized, the generalized masses have unit values $M_n = 1$ for $n = 1 \dots N_s$. Eq. (2) can then be applied to find FRFs for hydrodynamic pressure, and those for dam displacements and accelerations can be expressed as

$$\bar{u}(x, y, \omega) = \sum_{j=1}^{N_s} \psi_j^{(x)}(x, y) \bar{Z}_j(\omega); \quad \bar{\ddot{u}}(x, y, \omega) = -\omega^2 \sum_{j=1}^{N_s} \psi_j^{(x)}(x, y) \bar{Z}_j(\omega) \quad (15)$$

$$\bar{v}(x, y, \omega) = \sum_{j=1}^{N_s} \psi_j^{(y)}(x, y) \bar{Z}_j(\omega); \quad \bar{\ddot{v}}(x, y, \omega) = -\omega^2 \sum_{j=1}^{N_s} \psi_j^{(y)}(x, y) \bar{Z}_j(\omega) \quad (16)$$

where \bar{u} and \bar{v} denote the horizontal and vertical displacements, respectively, $\bar{\ddot{u}}$ and $\bar{\ddot{v}}$ the horizontal and vertical accelerations, respectively, $\psi_j^{(x)}$ and $\psi_j^{(y)}$ the x - and y -components of structural mode shape ψ_j , and N_s the number of structural mode shapes included in the analysis.

3 Simplified formulation

3.1 Fundamental mode response analysis

As described in the previous section, a rigorous analysis of a dam-reservoir system requires the determination of several structural mode shapes of the dam with an empty reservoir. To investigate most significant factors influencing dam seismic behavior, simplified procedures using only fundamental vibration mode response have been developed and proven efficient for preliminary dam design and safety evaluation [20]. Considering only the fundamental mode response, Eqs. (11) to (13) simplify to

$$\bar{Z}_1(\omega) = \frac{-L_1 - B_0(\omega)}{-\omega^2 \left(M_1 + \text{Re} [B_1(\omega)] \right) + i\omega \left(C_1 - \omega \text{Im} [B_1(\omega)] \right) + K_1} \quad (17)$$

where the generalized earthquake force coefficient L_1 , generalized mass M_1 , generalized damping C_1 , and generalized stiffness K_1 of the Equivalent Single Degree of Freedom (ESDOF) system of the dam with an empty reservoir are given by

$$L_1 = \psi_1^T \mathbf{M} \mathbf{1}; \quad M_1 = \psi_1^T \mathbf{M} \psi_1; \quad C_1 = 2\xi_1 \omega_1 M_1; \quad K_1 = \omega_1^2 M_1 \quad (18)$$

in which ξ_1 is the fraction of critical damping at the fundamental vibration mode ψ_1 of the dam with an empty reservoir, and ω_1 its fundamental vibration frequency. A finite element analysis can be conducted to obtain the generalized force L_1 and generalized mass M_1 from their discretized forms according to

Eq. (18). The following analytical expressions can also be used

$$L_1 = \iint \rho_s(x, y) \psi_1^{(x)}(x, y) \, dx dy \quad (19)$$

$$M_1 = \iint \rho_s(x, y) [\psi_1^{(x)}(x, y)]^2 \, dx dy + \iint \rho_s(x, y) [\psi_1^{(y)}(x, y)]^2 \, dx dy \quad (20)$$

in which ρ_s is the mass density of the dam concrete. These equations can be simplified by approximating the integration over the area of the dam by integration over its height [20] as

$$L_1 = \int_0^{H_s} \mu_s(y) \psi_1^{(x)}(0, y) \, dy; \quad M_1 = \int_0^{H_s} \mu_s(y) [\psi_1^{(x)}(0, y)]^2 \, dy \quad (21)$$

where μ_s is the mass of the dam per unit height.

The complex-valued hydrodynamic terms B_0 and B_1 in Eq. (17) can be expressed as

$$B_0(\omega) = - \int_0^{H_r} \bar{p}_0(0, y, \omega) \psi_1^{(x)}(0, y) \, dy = \sum_{n=1}^{N_r} B_{0n}(\omega) \quad (22)$$

$$B_1(\omega) = - \int_0^{H_r} \bar{p}_1(0, y, \omega) \psi_1^{(x)}(0, y) \, dy = \sum_{n=1}^{N_r} B_{1n}(\omega) \quad (23)$$

in which

$$B_{0n}(\omega) = - \int_0^{H_r} \bar{p}_{0n}(0, y, \omega) \psi_1^{(x)}(0, y) \, dy \quad (24)$$

$$B_{1n}(\omega) = - \int_0^{H_r} \bar{p}_{1n}(0, y, \omega) \psi_1^{(x)}(0, y) \, dy \quad (25)$$

These parameters account for the effects of dam-reservoir interaction. As can be seen from Eq. (17), the term B_0 can be interpreted as an added force, the real part of B_1 as an added mass and the imaginary part of B_1 as an added damping. Accordingly, Fenves and Chopra [7] showed that the seismic response of a dam-reservoir system can be approximated by evaluating the generalized coordinate \bar{Z}_1 at the natural vibration frequency ω_r of the dam-reservoir system. At this frequency, hydrodynamic pressures \bar{p}_0 , \bar{p}_1 and consequently hydrodynamic terms B_0 and B_1 are real, yielding from Eq. (17)

$$\bar{Z}_1(\omega_r) = \frac{-\tilde{L}_1}{-\omega_r^2 \tilde{M}_1 + i \omega_r \tilde{C}_1 + \omega_r^2 M_1} \quad (26)$$

where the generalized force \tilde{L}_1 , generalized mass \tilde{M}_1 and generalized damping \tilde{C}_1 of the dam-reservoir ESDOF system are obtained by modifying the parameters of the ESDOF system of the dam with an empty reservoir as follows

$$\tilde{L}_1 = L_1 + B_0(\omega_r) \quad (27)$$

$$\tilde{M}_1 = M_1 + \text{Re}[B_1(\omega_r)] = M_1 + B_1(\omega_r) \quad (28)$$

$$\tilde{C}_1 = C_1 - \omega_r \text{Im}[B_1(\omega_r)] = C_1 \quad (29)$$

From Eq. (29), we may deduce the equivalent damping ratio $\tilde{\xi}_r$ of the dam-reservoir ESDOF system as

$$\tilde{\xi}_r = \frac{\tilde{C}_1}{2\omega_r \tilde{M}_1} \quad (30)$$

To develop analytical expressions for determining the fundamental vibration period of the dam including the effects of impounded water, we assume that the x -component of the dam fundamental mode shape ψ_1 can be approximated as a cubic polynomial function

$$\psi_1^{(x)}(0, y) = a_1 \frac{y}{H_s} + a_2 \left(\frac{y}{H_s} \right)^2 + a_3 \left(\frac{y}{H_s} \right)^3 \quad (31)$$

where y is a coordinate varying along the height of the structure measured from its base. The coefficients a_1 , a_2 and a_3 can be determined based on a finite element analysis of the dam monolith as illustrated in Fig. 2, or using the fundamental mode shape of a standard gravity dam section proposed by Fenves and Chopra [19] as will be shown later.

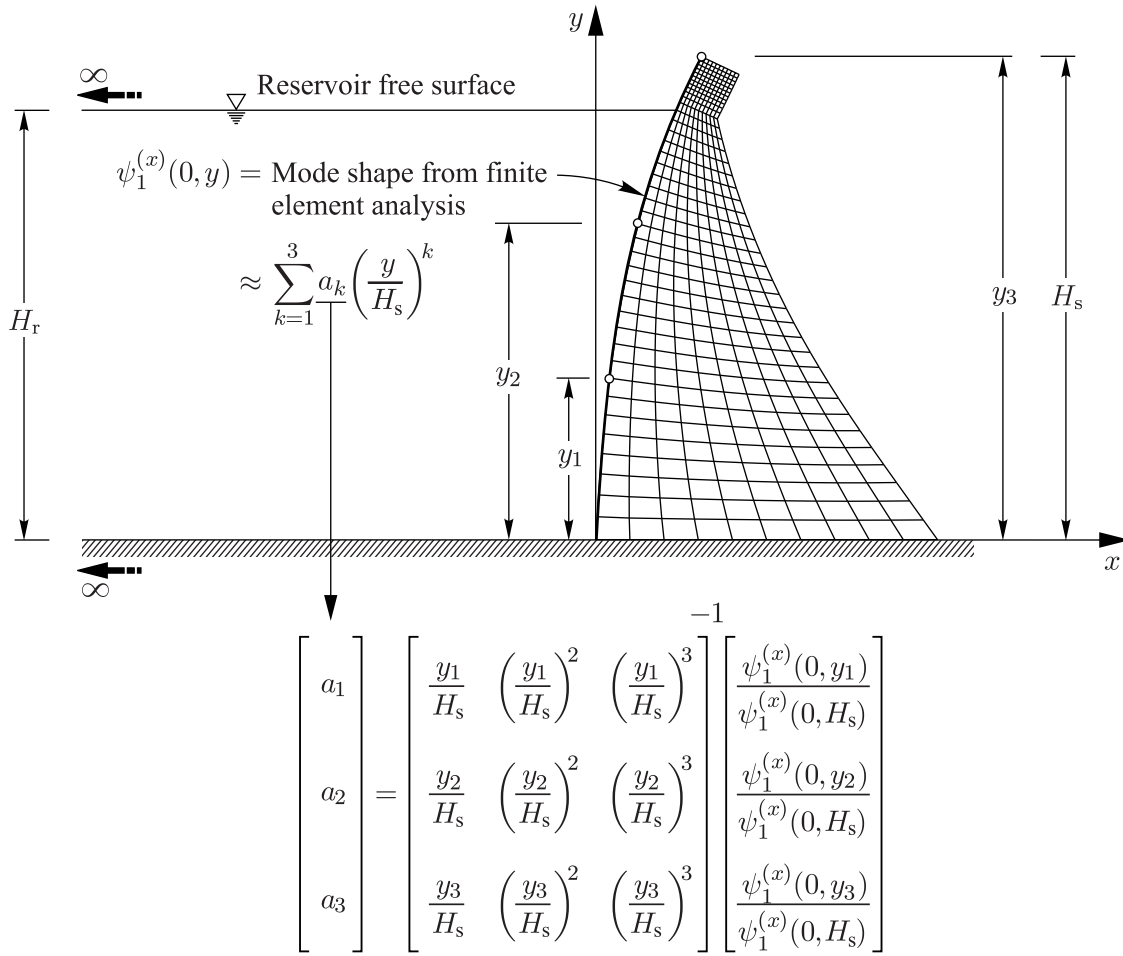


Figure 2. Approximation of the fundamental mode shape of a gravity dam.

3.2 Simplified formulation of dam-reservoir interaction assuming incompressible water

Introducing Eqs. (6), (9), (10) and (31) into Eqs. (22) and (23), we show that hydrodynamic terms B_{0n} and B_{1n} are real-valued and frequency-independent. They can be expressed as

$$\hat{B}_{0n} = 8\rho_r\eta^2 H_s^2 \frac{(-1)^n [2 \times (-1)^n F_n(\eta) - (2n-1)\pi G_n(\eta)]}{(2n-1)^3 \pi^3} \quad (32)$$

$$\hat{B}_{1n} = 4\rho_r\eta^2 H_s^2 \frac{[2 \times (-1)^n F_n(\eta) - (2n-1)\pi G_n(\eta)]^2}{(2n-1)^3 \pi^3} \quad (33)$$

where the hat sign indicates quantities corresponding to the incompressible water case, $\eta = H_r/H_s$ denotes the ratio of reservoir level to dam height, and where functions F_n and G_n are given by

$$F_n(\eta) = \eta a_1 + \left[1 - \frac{8}{(2n-1)^2 \pi^2}\right] \eta^2 a_2 + \left[1 - \frac{24}{(2n-1)^2 \pi^2}\right] \eta^3 a_3 \quad (34)$$

$$G_n(\eta) = -\frac{4\eta}{(2n-1)^2 \pi^2} \left[a_1 - \frac{24\eta^2}{(2n-1)^2 \pi^2} a_3 \right]$$

Eq. (17) simplifies then to

$$\bar{Z}_1(\omega) = \frac{-L_1 - \hat{B}_0}{-\omega^2(M_1 + \hat{B}_1) + i\omega C_1 + K_1} \quad (35)$$

It can be shown numerically that the generalized damping C_1 has little effect on the fundamental vibration frequency ω_r of the dam-reservoir system. Consequently, ω_r can be approximated as the excitation frequency corresponding to the resonance of the generalized coordinate \bar{Z}_1 in Eq. (35) with $C_1 = 0$, yielding

$$\omega_r^2(M_1 + \hat{B}_1) - K_1 = 0 \quad (36)$$

where

$$\hat{B}_1 = \sum_{n=1}^{N_r} \hat{B}_{1n} = 4\rho_r H_s^2 \Phi(\eta, N_r) \quad (37)$$

in which the function $\Phi(\eta, N_r)$ is defined by

$$\Phi(\eta, N_r) = \eta^2 \sum_{n=1}^{N_r} \frac{[2 \times (-1)^n F_n(\eta) - (2n-1)\pi G_n(\eta)]^2}{(2n-1)^3 \pi^3} \quad (38)$$

A sufficient number N_r of reservoir modes should be included to determine the sum Φ in Eq. (38). Figure 3 illustrates the variation of Φ as a function of reservoir height ratio η and number of included reservoir modes N_r . We show numerically that the sum Φ converges towards a function $\hat{\varphi}$ depending only on reservoir height ratio η

$$\begin{aligned} \lim_{N_r \rightarrow +\infty} \Phi(\eta, N_r) &= \eta^4 \left[\hat{\gamma}_1 a_1^2 + \hat{\gamma}_2 a_1 a_2 \eta + (\hat{\gamma}_3 a_2^2 + \hat{\gamma}_4 a_1 a_3) \eta^2 + \hat{\gamma}_5 a_2 a_3 \eta^3 + \hat{\gamma}_6 a_3^2 \eta^4 \right] \\ &= \hat{\varphi}(\eta) \end{aligned} \quad (39)$$

where coefficients $\hat{\gamma}_1$ to $\hat{\gamma}_6$ are given in Table 1.

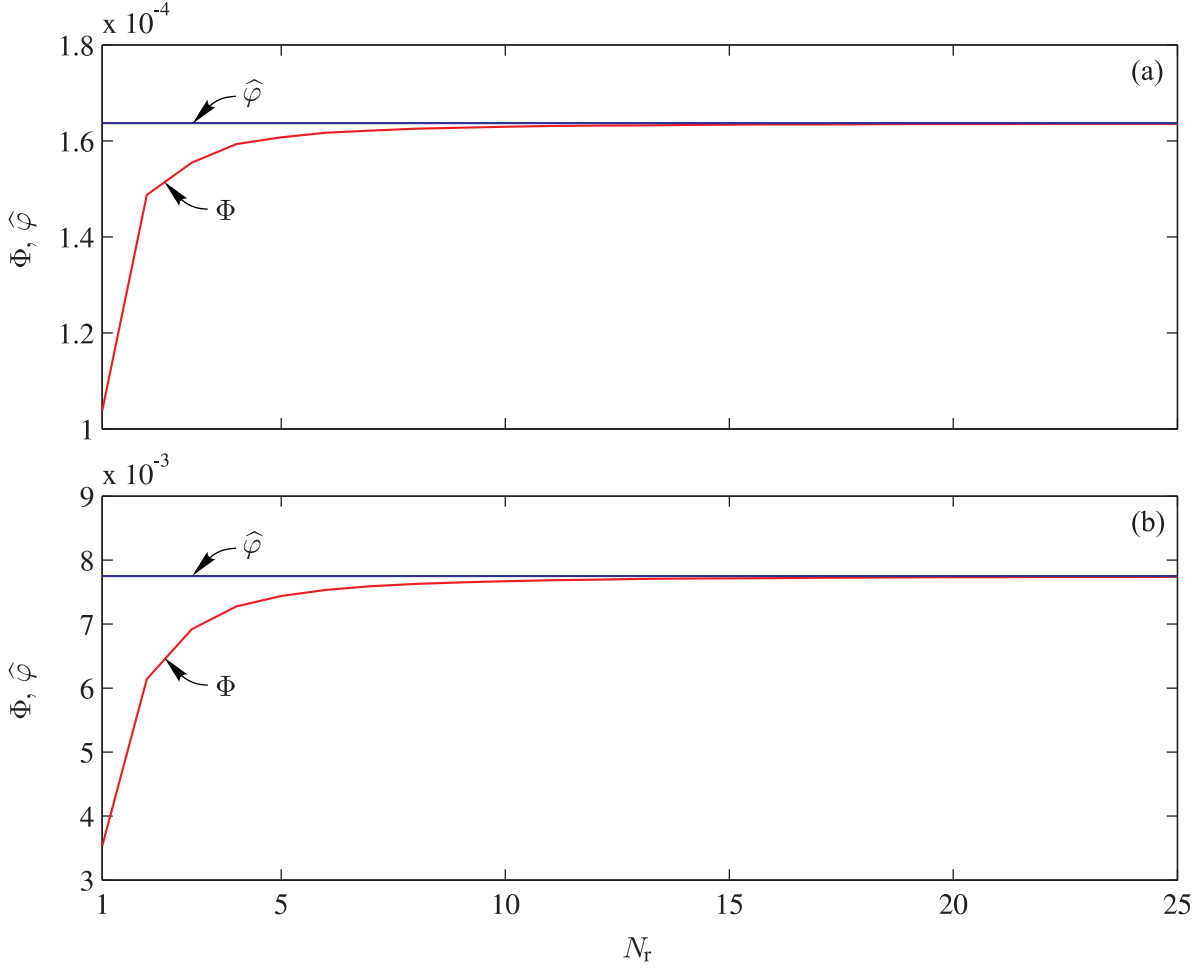


Figure 3. Variation of Φ and $\hat{\Phi}$ as a function of reservoir height ratio η and number of included reservoir modes N_r : (a) $\eta = 0.50$ and (b) $\eta = 1.00$.

The limit $\hat{\Phi}$ is also shown in Fig. 3. Replacing into Eq. (36) yields the fundamental resonant frequency and period of a dam-reservoir system with water compressibility neglected

$$\omega_r = \frac{\omega_1}{\sqrt{1 + \frac{4\rho_r H_s^2 \hat{\Phi}(\eta)}{M_1}}}; \quad T_r = T_1 \sqrt{1 + \frac{4\rho_r H_s^2 \hat{\Phi}(\eta)}{M_1}} \quad (40)$$

where T_1 denotes the fundamental vibration period of the dam with an empty reservoir.

To obtain a simplified expression of the generalized coordinate \bar{Z}_1 of the dam-reservoir system at resonant frequency ω_r , a simplified expression of the hydrodynamic term \hat{B}_0 has to be found. When water

Table 1. Coefficients $\hat{\gamma}_i$ and γ_i , $i = 1, \dots, 6$.

Incompressible water	Compressible water
$\hat{\gamma}_1 = 25.769 \times 10^{-3}$	$\gamma_1 = 8.735 \times 10^{-3}$
$\hat{\gamma}_2 = 31.820 \times 10^{-3}$	$\gamma_2 = 14.059 \times 10^{-3}$
$\hat{\gamma}_3 = 10.405 \times 10^{-3}$	$\gamma_3 = 5.776 \times 10^{-3}$
$\hat{\gamma}_4 = 22.082 \times 10^{-3}$	$\gamma_4 = 11.172 \times 10^{-3}$
$\hat{\gamma}_5 = 15.031 \times 10^{-3}$	$\gamma_5 = 9.343 \times 10^{-3}$
$\hat{\gamma}_6 = 5.587 \times 10^{-3}$	$\gamma_6 = 3.840 \times 10^{-3}$

compressibility is neglected, we have according to Eq. (32)

$$\hat{B}_0 = \sum_{n=1}^{N_r} \hat{B}_{0n} = 8\rho_r H_s^2 \Theta(\eta, N_r) \quad (41)$$

where the function $\Theta(\eta, N_r)$ is given by

$$\Theta(\eta, N_r) = \eta^2 \sum_{n=1}^{N_r} \frac{(-1)^{n-1} [2 \times (-1)^{n-1} F_n(\eta) + (2n-1) \pi G_n(\eta)]}{(2n-1)^3 \pi^3} \quad (42)$$

As for the function Φ , we show numerically that the sum Θ converges towards a function $\hat{\theta}$ depending only on reservoir height ratio η

$$\lim_{N_r \rightarrow +\infty} \Theta(\eta, N_r) = \eta^3 (\hat{\zeta}_1 a_1 + \hat{\zeta}_2 a_2 \eta + \hat{\zeta}_3 a_3 \eta^2) = \hat{\theta}(\eta) \quad (43)$$

where the coefficients $\hat{\zeta}_1$ to $\hat{\zeta}_3$ are given in Table 2. The hydrodynamic term \hat{B}_0 can then be approximated as

$$\hat{B}_0 = 8\rho_r H_s^2 \hat{\theta}(\eta) \quad (44)$$

Table 2. Coefficients $\hat{\zeta}_i$ and ζ_i , $i = 1, 2, 3$.

Incompressible water	Compressible water
$\hat{\zeta}_1 = 27.234 \times 10^{-3}$	$\zeta_1 = 3.795 \times 10^{-3}$
$\hat{\zeta}_2 = 15.323 \times 10^{-3}$	$\zeta_2 = 3.105 \times 10^{-3}$
$\hat{\zeta}_3 = 10.006 \times 10^{-3}$	$\zeta_3 = 2.500 \times 10^{-3}$

Neglecting the influence of damping on the fundamental vibration frequency ω_r of the dam-reservoir system and using the analytical expressions developed above, the properties given in Eqs. (27), (28)

and (30) to characterize the dam-reservoir ESDOF system can now be obtained as

$$\tilde{L}_1 = L_1 + 8\rho_r H_s^2 \hat{\theta}(\eta) \quad (45)$$

$$\tilde{M}_1 = M_1 + 4\rho_r H_s^2 \hat{\varphi}(\eta) = \frac{\omega_1^2}{\omega_r^2} M_1 \quad (46)$$

$$\tilde{\xi}_1 = \frac{C_1}{2\omega_r \tilde{M}_1} = \frac{\omega_r}{\omega_1} \xi_1 \quad (47)$$

3.3 Simplified formulation of dam-reservoir interaction considering water compressibility

Introducing Eqs. (4) to (6) and Eq. (31) into Eqs. (22) and (23), we show that the hydrodynamic terms B_{0n} and B_{1n} are now complex-valued and frequency-dependent, and that they can be expressed as

$$B_{0n}(\omega) = 4\rho_r \eta H_s \frac{(-1)^n \left[2 \times (-1)^n F_n(\eta) - (2n-1) \pi G_n(\eta) \right]}{(2n-1)^2 \pi^2 \sqrt{\frac{(2n-1)^2 \pi^2}{4\eta^2 H_s^2} - \frac{\omega^2}{C_r^2}}} \quad (48)$$

$$B_{1n}(\omega) = 2\rho_r \eta H_s \frac{\left[2 \times (-1)^n F_n(\eta) - (2n-1) \pi G_n(\eta) \right]^2}{(2n-1)^2 \pi^2 \sqrt{\frac{(2n-1)^2 \pi^2}{4\eta^2 H_s^2} - \frac{\omega^2}{C_r^2}}} \quad (49)$$

As mentioned previously, the fundamental vibration frequency ω_r of the dam-reservoir system can be approximated as the frequency corresponding to the resonance of the generalized coordinate \bar{Z}_1 in Eq. (17) with $C_1 = 0$, yielding in this case

$$\omega_r^2 \left[M_1 + B_1(\omega_r) \right] - K_1 = 0 \quad (50)$$

Eq. (50) is more difficult to solve than Eq. (36) obtained assuming incompressible water, since the term B_1 is now frequency-dependent. To circumvent this difficulty, we show that we can approximate the value of hydrodynamic term B_1 at the resonant frequency ω_r as

$$B_1(\omega_r) = B_{1,1}(\omega_r) + \sum_{n=2}^{N_r} B_{1n}(0) \quad (51)$$

where $B_{1,1}(\omega_r)$ is given by

$$B_{1,1}(\omega_r) = 4\rho_r \eta^2 H_s^2 \frac{\left[2F_1(\eta) + \pi G_1(\eta) \right]^2}{\pi^3 \sqrt{1 - \frac{\omega_r^2}{\omega_0^2}}} \quad (52)$$

in which $\omega_0 = \pi C_r / (2H_r)$ denotes the fundamental vibration frequency of the full reservoir, and where F_1 and G_1 can be obtained from Eq. (34) with $n=1$

$$\begin{aligned} F_1(\eta) &= \eta a_1 + \left(1 - \frac{8}{\pi^2}\right) \eta^2 a_2 + \left(1 - \frac{24}{\pi^2}\right) \eta^3 a_3 \\ G_1(\eta) &= -\frac{4\eta}{\pi^2} \left(a_1 - \frac{24\eta^2}{\pi^2} a_3\right) \end{aligned} \quad (53)$$

The value of B_{1n} at $\omega=0$ is given by Eq. (49)

$$B_{1n}(0) = 4\rho_r \eta^2 H_s^2 \frac{[2 \times (-1)^n F_n(\eta) - (2n-1) \pi G_n(\eta)]^2}{(2n-1)^3 \pi^3} \quad (54)$$

Eq. (51) can then be rewritten as

$$B_1(\omega_r) = B_{1,1}(\omega_r) + 4\rho_r H_s^2 \left\{ \Phi(\eta, N_r) - \frac{\eta^2}{\pi^3} [2F_1(\eta) + \pi G_1(\eta)]^2 \right\} \quad (55)$$

where $\Phi(\eta, N_r)$ is given by Eq. (38). Considering the limit as $N_r \rightarrow +\infty$, we find that

$$B_1(\omega_r) = B_{1,1}(\omega_r) + 4\rho_r H_s^2 \varphi(\eta) \quad (56)$$

in which

$$\begin{aligned} \varphi(\eta) &= \lim_{N_r \rightarrow +\infty} \Phi(\eta, N_r) - \frac{\eta^2}{\pi^3} [2F_1(\eta) + \pi G_1(\eta)]^2 \\ &= \hat{\varphi}(\eta) - \frac{\eta^2}{\pi^3} [2F_1(\eta) + \pi G_1(\eta)]^2 \\ &= \eta^4 \left[\gamma_1 a_1^2 + \gamma_2 a_1 a_2 \eta + (\gamma_3 a_2^2 + \gamma_4 a_1 a_3) \eta^2 + \gamma_5 a_2 a_3 \eta^3 + \gamma_6 a_3^2 \eta^4 \right] \end{aligned} \quad (57)$$

We note that $\varphi(\eta)$ has the same expression as $\hat{\varphi}(\eta)$ in Eq. (39), but with coefficients γ_1 to γ_6 corresponding to the compressible water case as indicated in Table 1. To validate Eq. (56), Fig. 4 compares the term $4\rho_r H_s^2 \varphi(\eta)$ to the real and imaginary parts of the hydrodynamic term ($B_1 - B_{1,1}$) determined at frequency ratios ω/ω_0 varying from 0 to 4. As can be seen, the approximation in Eq. (56) is valid for frequency ratios ω/ω_0 up to 1, and a fortiori for the dam-reservoir fundamental frequency ω_r , since $\omega_r/\omega_0 < 1$. Substituting Eq. (56) into Eq. (50) and introducing the frequency ratios $R_r = \omega_r/\omega_0$ and $R_1 = \omega_1/\omega_0$, we show that Eq. (50) can be rewritten under the form of a cubic equation to be solved for $\chi = R_r^2$

$$A_1 \chi^3 + A_2 \chi^2 + A_3 \chi + A_4 = 0 \quad (58)$$

where

$$A_0 = 1 + \frac{4\rho_r H_s^2 \varphi(\eta)}{M_1} \quad (59)$$

$$A_1 = A_0^2 \quad (60)$$

$$A_2 = -A_0 (A_0 + 2R_1^2) + \left\{ \frac{4\rho_r \eta^2 H_s^2}{M_1 \pi^3} [2F_1(\eta) + \pi G_1(\eta)]^2 \right\}^2 \quad (61)$$

$$A_3 = R_1^2 (2A_0 + R_1^2) \quad (62)$$

$$A_4 = -R_1^4 \quad (63)$$

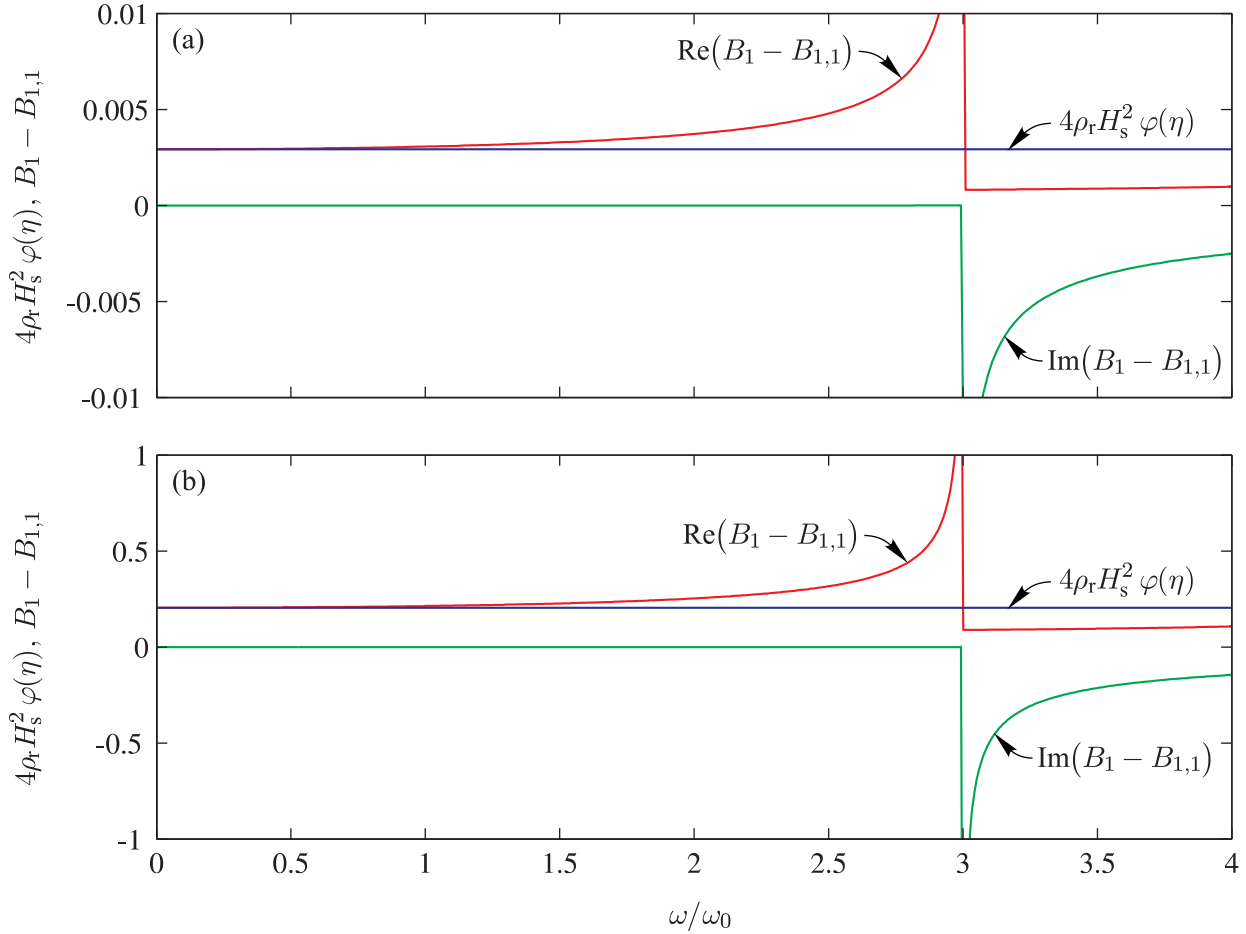


Figure 4. Variation of the terms $4\rho_r H_s^2 \varphi(\eta)$ and $(B_1 - B_{1,1})$ as a function of frequency ratio ω/ω_0 and reservoir height ratio η : (a) $\eta = 0.50$ and (b) $\eta = 1.00$.

The fundamental vibration frequency $\omega_r = \omega_0 R_r$ and period $T_r = 2\pi/\omega_r$ of the dam-reservoir system can then be obtained by solving Eq. (58) numerically or analytically using Cardano's formula. In the latter case, Eq. (58) can be first reduced to

$$\Gamma^3 + D_1 \Gamma + D_2 = 0 \quad (64)$$

where

$$\Gamma = \chi + \frac{1}{3} \frac{A_2}{A_1}; \quad D_1 = \frac{A_3}{A_1} - \frac{1}{3} \left(\frac{A_2}{A_1} \right)^2; \quad D_2 = \frac{2}{27} \left(\frac{A_2}{A_1} \right)^3 - \frac{A_2 A_3}{3A_1^2} + \frac{A_4}{A_1} \quad (65)$$

Eq. (64) has three solutions Γ_1 , Γ_2 and Γ_3 that can be expressed as [25]

$$\Gamma_1 = U + V; \quad \Gamma_2 = \tau U + \tau^2 V; \quad \Gamma_3 = \tau^2 U + \tau V \quad (66)$$

where

$$U = \left(-\frac{D_2}{2} + \sqrt{\Delta} \right)^{1/3}; \quad V = -\frac{1}{3} \frac{D_1}{U}; \quad \tau = -\frac{1}{2} + i \frac{\sqrt{3}}{2} \quad (67)$$

and where Δ denotes the discriminant

$$\Delta = \left(\frac{D_1}{3} \right)^3 + \left(\frac{D_2}{2} \right)^2 \quad (68)$$

We denote as Γ^* the only real solution among Γ_1 , Γ_2 and Γ_3 that satisfies

$$\frac{A_2}{3A_1} \leq \Gamma^* \leq R_1^2 + \frac{A_2}{3A_1} \quad (69)$$

The frequency ratio R_r and fundamental vibration period T_r of the dam-reservoir system are then given by

$$R_r = \frac{\omega_r}{\omega_0} = \sqrt{\Gamma^* - \frac{A_2}{3A_1}}; \quad T_r = \frac{2\pi}{\omega_0 \sqrt{\Gamma^* - \frac{A_2}{3A_1}}} \quad (70)$$

Once the vibration frequency ω_r is known, we can determine the properties of the dam-reservoir ESDOF system as described in the previous section for the case of incompressible water. When water compressibility is included, we show that the hydrodynamic term $B_0(\omega_r)$ can be expressed as

$$B_0(\omega_r) = B_{0,1}(\omega_r) + \sum_{n=2}^{N_r} B_{0n}(0) \quad (71)$$

where $B_{0,1}(\omega_r)$ is given by

$$B_{0,1}(\omega_r) = 8\rho_r \eta^2 H_s^2 \frac{[2F_1(\eta) + \pi G_1(\eta)]}{\pi^3 \sqrt{1 - R_r^2}} \quad (72)$$

and where the value of B_{0n} at $\omega = 0$ is obtained from Eq. (48)

$$B_{0n}(0) = 8\rho_r \eta^2 H_s^2 \frac{[2 \times (-1)^{n-1} F_n(\eta) + (2n-1) \pi G_n(\eta)]}{(2n-1)^3 \pi^3} \quad (73)$$

Eq. (71) can then be rewritten as

$$B_0(\omega_r) = B_{0,1}(\omega_r) + 8\rho_r H_s^2 \left\{ \Theta(\eta, N_r) - \frac{\eta^2}{\pi^3} [2F_1(\eta) + \pi G_1(\eta)] \right\} \quad (74)$$

where $\Theta(\eta, N_r)$ is given by Eq. (42). Considering the limit as $N_r \rightarrow +\infty$, we find that

$$B_0(\omega_r) = B_{0,1}(\omega_r) + 8\rho_r H_s^2 \theta(\eta) \quad (75)$$

in which

$$\begin{aligned} \theta(\eta) &= \lim_{N_r \rightarrow +\infty} \Theta(\eta, N_r) - \frac{\eta^2}{\pi^3} \left[2F_1(\eta) + \pi G_1(\eta) \right] \\ &= \hat{\theta}(\eta) - \frac{\eta^2}{\pi^3} \left[2F_1(\eta) + \pi G_1(\eta) \right] \\ &= \eta^3 \left(\zeta_1 a_1 + \zeta_2 a_2 \eta + \zeta_3 a_3 \eta^2 \right) \end{aligned} \quad (76)$$

where coefficients ζ_1 to ζ_3 are given in Table 2. Neglecting the influence of damping on the fundamental vibration frequency of the dam-reservoir system and using the analytical expressions developed above, Eqs. (27), (28) and (30) become when water compressibility is included

$$\tilde{L}_1 = L_1 + 8\rho_r H_s^2 \left\{ \theta(\eta) + \eta^2 \frac{[2F_1(\eta) + \pi G_1(\eta)]}{\pi^3 \sqrt{1 - R_r^2}} \right\} \quad (77)$$

$$\tilde{M}_1 = M_1 + 4\rho_r H_s^2 \left\{ \varphi(\eta) + \eta^2 \frac{[2F_1(\eta) + \pi G_1(\eta)]^2}{\pi^3 \sqrt{1 - R_r^2}} \right\} = \frac{\omega_1^2}{\omega_r^2} M_1 \quad (78)$$

$$\tilde{\xi}_1 = \frac{\omega_r}{\omega_1} \xi_1 \quad (79)$$

3.4 Application to the simplified earthquake analysis of gravity dams

The maximum response of a dam-reservoir ESDOF system to a horizontal earthquake ground motion can be approximated by its static response under the effect of equivalent lateral forces f_1 applied at the dam upstream face and expressed per unit dam height as [20, 26]

$$\begin{aligned} f_1(y) &= \frac{\tilde{L}_1}{\tilde{M}_1} S_a(T_r, \tilde{\xi}_1) \left\{ \mu_s(y) \psi_1^{(x)}(0, y) - \bar{p}_1(0, y, \omega_r) \right\} \\ &= \frac{\tilde{L}_1}{\tilde{M}_1} S_a(T_r, \tilde{\xi}_1) \left[\mu_s(y) \left(a_1 \frac{y}{H_s} + a_2 \frac{y^2}{H_s^2} + a_3 \frac{y^3}{H_s^3} \right) - \bar{p}_1(0, y, \omega_r) \right] \end{aligned} \quad (80)$$

where $S_a(T_r, \tilde{\xi}_1)$ is the pseudo-acceleration ordinate of the earthquake design spectrum at vibration period T_r and for damping ratio $\tilde{\xi}_1$ of the dam-reservoir ESDOF system described previously, and where the

hydrodynamic pressure $\bar{p}_1(0, y, \omega_r)$ can be expressed using a cubic mode shape approximation as

$$\bar{p}_1(0, y, \omega_r) = 2\rho_r \sum_{n=1}^{N_r} \frac{2 \times (-1)^n F_n(\eta) - (2n-1)\pi G_n(\eta)}{(2n-1)\pi \sqrt{\frac{(2n-1)^2 \pi^2}{4\eta^2 H_s^2} - \frac{\omega_r^2}{C_r^2}}} \cos \left[\frac{(2n-1)\pi}{2H_r} y \right] \quad (81)$$

in which F_n and G_n are given by Eq. (34), and the ratio of generalized force \tilde{L}_1 to generalized mass \tilde{M}_1 is obtained from Eqs. (77) and (78). If water compressibility is neglected, Eq. (81) simplifies to

$$\bar{p}_1(0, y, \omega_r) = 4\rho_r \eta H_s \sum_{n=1}^{N_r} \frac{2 \times (-1)^n F_n(\eta) - (2n-1)\pi G_n(\eta)}{(2n-1)^2 \pi^2} \cos \left[\frac{(2n-1)\pi}{2H_r} y \right] \quad (82)$$

with \tilde{L}_1 and \tilde{M}_1 to be determined using Eqs. (45) and (46). We note that the minus sign in Eq. (80) corresponds to the orientation of the system of axes shown in Fig. 5. We also assume that the fundamental mode shape component $\psi_1^{(x)}$ is positive as indicated on the same Figure.

Fenves and Chopra [19,20] discussed the effects of higher vibration modes on dam earthquake response. Using a static correction technique, this effect can be accounted for approximately by evaluating the static response of the dam-reservoir ESDOF subjected to the lateral forces f_{sc} applied at the dam upstream face and expressed per unit dam height as

$$f_{sc}(y) = \ddot{x}_g^{(\max)} \left\{ \mu_s(y) \left[1 - \frac{L_1}{M_1} \psi_1^{(x)}(0, y) \right] - \left[\hat{p}_0(0, y) + \frac{\mu_s(y)}{M_1} \psi_1^{(x)}(0, y) \int_0^{H_r} \hat{p}_0(0, y) \psi_1^{(x)}(0, y) dy \right] \right\} \quad (83)$$

where $\ddot{x}_g^{(\max)}$ denotes the maximum ground acceleration, and $\hat{p}_0(0, y)$ the real-valued, frequency-independent hydrodynamic pressure applied on a rigid dam subjected to a unit ground acceleration and impounding an incompressible water reservoir given by

$$\hat{p}_0(0, y) = \frac{8\rho_r \eta H_s}{\pi^2} \sum_{n=1}^{N_r} \frac{(-1)^n}{(2n-1)^2} \cos \left[\frac{(2n-1)\pi}{2\eta H_s} y \right] \quad (84)$$

Assuming a cubic mode approximation, we show that Eq.(83) can be rewritten as

$$f_{sc}(y) = \ddot{x}_g^{(\max)} \left\{ \mu_s(y) \left(1 - \left[\frac{L_1}{M_1} + 8\rho_r H_s^2 \frac{\hat{\theta}(\eta)}{M_1} \right] \left[a_1 \frac{y}{H_s} + a_2 \frac{y^2}{H_s^2} + a_3 \frac{y^3}{H_s^3} \right] \right) - \hat{p}_0(0, y) \right\} \quad (85)$$

The total earthquake response of the dam can then be determined by applying the SRSS rule to combine response quantities associated with the fundamental and higher vibration modes [19,20].

4 Dam models, analyses and results

4.1 Analyses conducted

In this section, we assess the effectiveness of the equations developed above in determining the fundamental mode response of gravity dams. To illustrate the analysis types conducted, we consider a dam section with dimensions inspired from the tallest non-overflow monolith of Pine Flat dam [15]. The dam cross-section is shown in Fig. 5 (a).

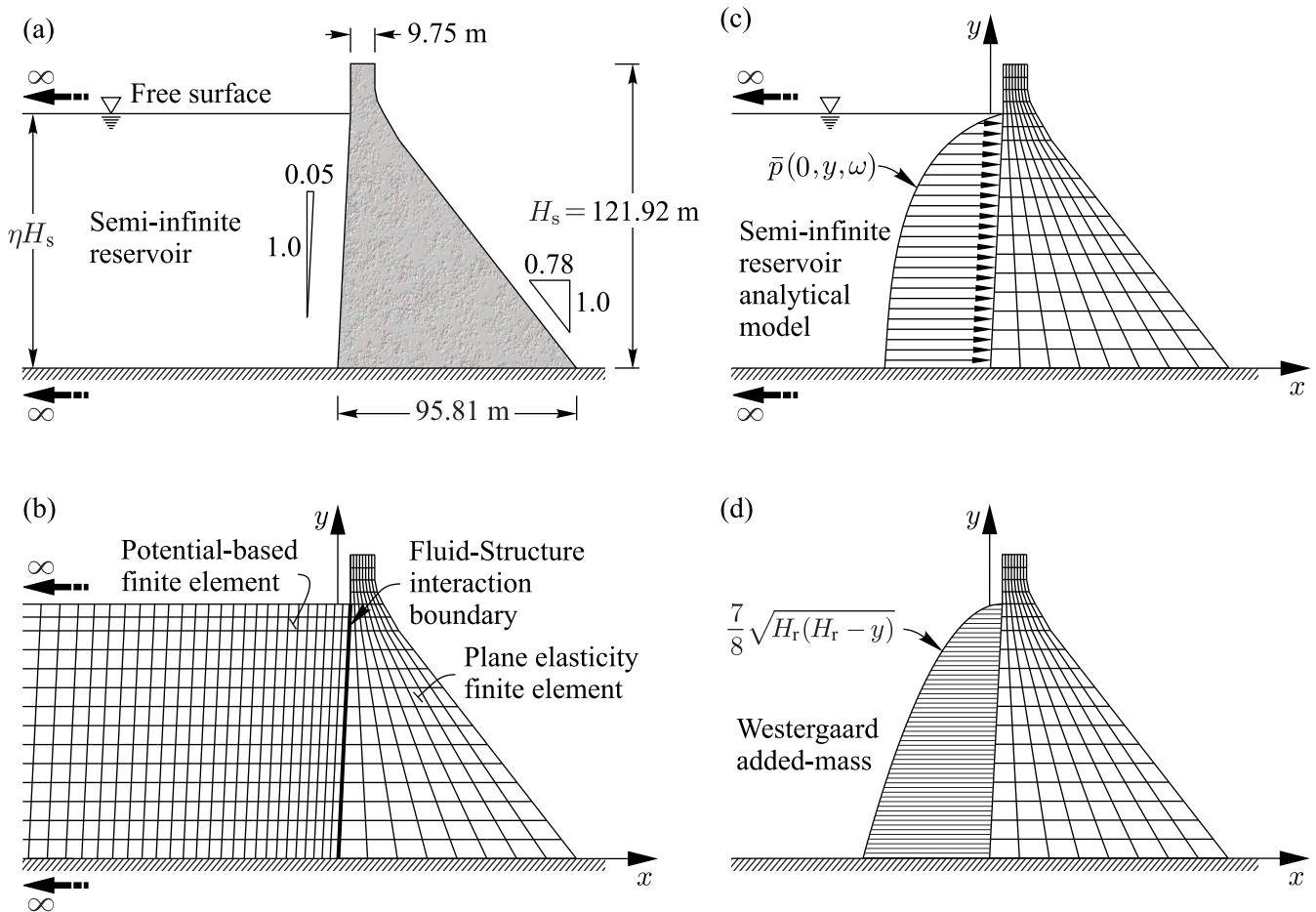


Figure 5. (a) Dam-reservoir system geometry; (b) Analysis type I: Finite element model; (c) Analysis type II: analytical solution; (d) Analysis type III: Westergaard added mass formulation.

The following six types of analysis are conducted to determine the fundamental vibration frequency of the dam-reservoir system:

- Analysis type I: a finite element analysis where both the dam and the reservoir are modeled using finite elements. The software ADINA [27] is used to discretize the dam monolith into 9-node plane stress finite elements. The reservoir is truncated at a large distance of $20H_r$ from the dam upstream face to eliminate reflection of waves at the far reservoir upstream end. The 9-node potential-based finite

elements programmed in ADINA [27] are used to model the reservoir. Fluid-structure interaction is accounted for through special interface elements also included in the software. A finite element model of the dam-reservoir system is shown in Fig. 5 (d). The performance of the potential-based formulation and the fluid-structure interface elements was assessed in a previous work [24]. The method can accurately account for fluid-structure interaction in dam-reservoir systems with a general geometry, including when the dam upstream face is not vertical, which is for example the case of the slightly inclined upstream face of the Pine Flat dam section. The results of this analysis will serve as our reference solution in the rest of the paper.

- Analysis type II: the analytical solution originally developed by Fenves and Chopra [7] and reviewed in section 2. The same 9-node plane stress finite element model built for Type I analysis is used as illustrated in Fig. 5 (c). The structural frequency response of the dam including hydrodynamic effects is then determined using Eqs. (2) to (16). The fundamental frequency is identified next as that corresponding to the first resonant structural response.
- Analysis type III: a finite element analysis of the Pine Flat dam where the reservoir hydrodynamic loading is modeled approximately using Westergaard added mass formulation, assuming a rigid dam with a vertical upstream face, impounding incompressible water [1]. The effect of the reservoir is equivalent in this case to inertia forces generated by a body of water of parabolic shape moving back and forth with the vibrating dam. The finite element model of the dam and the body of water are shown in Fig. 5 (d). The added masse m_i to be attached to a node i belonging to dam-reservoir interface can be written as

$$m_i = \frac{7}{8} \rho_r V_i \sqrt{H_r(H_r - y_i)} \quad (86)$$

where y_i denotes the height of node i above the dam base and V_i the volume of water tributary to node i . As previously, the software ADINA [27] is used to discretize the dam monolith into 9-node plane stress finite elements.

- Analysis type IV: the new procedure proposed in this paper is applied using approximate parameters L_1 , M_1 , ω_1 and $\psi_1^{(x)}$ proposed by Fenves and Chopra [19, 20]. The authors analyzed several standard dam cross-sections and obtained the following conservative approximations for preliminary design purposes: $L_1 = 0.13 M_s$ and $M_1 = 0.043 M_s$, where M_s is the total mass of the dam monolith. Fenves and Chopra [19, 20] also proposed to estimate the fundamental vibration frequency ω_1 and period T_1 of the dam with an empty reservoir as

$$\omega_1 = \frac{2\pi\sqrt{E_s}}{0.38 H_s}; \quad T_1 = \frac{0.38 H_s}{\sqrt{E_s}} \quad (87)$$

where the dam concrete modulus of elasticity E_s is expressed in MPa and H_s in meters to yield ω_1 in rad/s and T_1 in seconds. To develop a simplified earthquake analysis procedure, Fenves and Chopra [19, 20] used the standard fundamental mode shape given in Table 3. Applying the procedure illustrated in

Fig. 2, this standard mode shape can be approximated using three points at elevations $y_1 = H_s/3$, $y_2 = 2H_s/3$ and $y_3 = H_s$, yielding the coefficients $a_1 = 0.3535$, $a_2 = -0.5455$ and $a_3 = 1.1920$. Eq. (31) becomes then

$$\psi_1^{(x)}(0, y) = 0.3535 \frac{y}{H_s} - 0.5455 \left(\frac{y}{H_s} \right)^2 + 1.1920 \left(\frac{y}{H_s} \right)^3 \quad (88)$$

The resulting cubic interpolation is shown in Table 3. When water compressibility is neglected, Eq. (39) simplifies to

$$\hat{\varphi}(\eta) = \eta^4 [7.938 \eta^4 - 9.774 \eta^3 + 12.400 \eta^2 - 6.136 \eta + 3.220] \times 10^{-3} \quad (89)$$

after replacing the coefficients a_1 to a_3 by their values. Introducing $M_1 = 0.043 M_s$ and substituting Eqs. (87) and (89) into Eq. (40) yields the dam-reservoir fundamental vibration frequency ω_r and period T_r when water compressibility is neglected. For example, considering a full reservoir, i.e. $\eta = 1$, we obtain

$$\omega_r = \frac{\omega_1}{\sqrt{1 + \frac{711.6 H_s^2}{M_s}}}; \quad T_r = T_1 \sqrt{1 + \frac{711.6 H_s^2}{M_s}} \quad (90)$$

When water compressibility is included, replacing the coefficients a_1 to a_3 by their values into Eqs. (53) and (57) yields

$$\varphi(\eta) = \eta^4 [5.456 \eta^4 - 6.075 \eta^3 + 6.426 \eta^2 - 2.711 \eta + 1.091] \times 10^{-3} \quad (91)$$

$$F_1(\eta) = 0.3535 \eta - 0.1033 \eta^2 - 1.7065 \eta^3 \quad (92)$$

$$G_1(\eta) = -0.1433 \eta + 1.1748 \eta^3 \quad (93)$$

The frequency ratio R_1 can be approximated as

$$R_1 = \frac{\omega_1}{\omega_0} = \frac{4\eta\sqrt{E_s}}{0.38 C_r} \quad (94)$$

Coefficients A_0 to A_4 can be obtained using $M_1 = 0.043 M_s$ and substituting Eqs. (91) to (94) into Eqs. (59) to (63). Eq. (58) is then solved for $\chi = R_r^2$ to obtain the fundamental vibration frequency $\omega_r = \omega_0 R_r$ and period $T_r = 2\pi/\omega_r$ of the dam-reservoir system.

- Analysis type V: the new procedure proposed in this paper is applied using the approximate parameters L_1 , M_1 and $\psi_1^{(x)}$ proposed by Fenves and Chopra [19, 20], but with the natural frequency ω_1 obtained from a finite element analysis. All the equations described in the previous analysis Type IV apply except for the frequency ratio R_1 which now results from finite element analysis.
- Analysis type VI: the new procedure proposed in this paper is applied using parameters L_1 , M_1 , $\psi_1^{(x)}$ and ω_1 obtained from a finite element analysis of the dam section with an empty reservoir. A fundamental mode shape normalized with respect to the mass of the dam can be used, yielding a generalized

mass $M_1 = 1$. Applying the procedure illustrated in Fig. 2, the fundamental mode shape evaluated at dam upstream face is interpolated using three points at elevations $y_1 = H_s/3$, $y_2 = 2H_s/3$ and $y_3 = H_s$ to find the coefficients a_1 to a_3 in Eq. (31). Table 3 contains the original mode shape resulting from finite element analysis of Pine Flat dam section as well as the cubic interpolation used. When water compressibility is neglected, the resulting coefficients are introduced into Eq. (39) to obtain $\hat{\varphi}(\eta)$ and then the dam-reservoir vibration frequency ω_r using the generalized mass M_1 and the fundamental vibration frequency ω_1 obtained from finite element analysis of the dam with an empty reservoir. When water compressibility is included, coefficients a_1 to a_3 are introduced into Eqs. (57) and (53) to obtain the parameters $\varphi(\eta)$, $F_1(\eta)$ and $G_1(\eta)$. Coefficients A_0 to A_4 are determined next and Eq. (58) is then solved for $\chi = R_r^2$ to obtain the vibration frequency of the dam-reservoir system as described in section 3.

4.2 Validation of the proposed simplified formulation

The six analysis types described in the previous section are carried out to assess the effectiveness of the method proposed in this paper. The Pine Flat dam section described previously is studied first. A mass density $\rho_s = 2400 \text{ kg/m}^3$ and a Poisson's ratio $\nu = 0.2$ are assumed as concrete material properties. To examine the influence of dam stiffness, two moduli of elasticity $E_s = 25 \text{ GPa}$ and $E_s = 35 \text{ GPa}$ are considered. A water mass density $\rho_r = 1000 \text{ kg/m}^3$ is adopted. Both compressible and incompressible water assumptions are investigated, with a pressure wave velocity of $C_r = 1440 \text{ m/s}$ in the former case. We compute the period ratios T_r/T_1 where T_r is the fundamental vibration period of the dam-reservoir system obtained using any of the six analysis types described previously, and T_1 is the reference fundamental vibration period determined using a finite element analysis of the dam with an empty reservoir. Figures 6 and 7 illustrate the period ratios T_r/T_1 obtained considering incompressible and compressible water assumptions, respectively. Results for reservoir height ratios from $\eta = 0.5$ to 1.0 and two moduli of elasticity $E_s = 25 \text{ GPa}$ and $E_s = 35 \text{ GPa}$ are given. Figures 6 and 7 also show bar charts representing the following error estimator

$$\varepsilon = \frac{T_r - T_r^{(\text{FE})}}{T_r^{(\text{FE})}} \quad (95)$$

where $T_r^{(\text{FE})}$ denotes the reference fundamental vibration period obtained using a finite element analysis of the dam-reservoir system, i.e. analysis type I.

First, it is apparent from the curves that the fundamental period predicted using finite elements, i.e. analysis type I, and the analytical formulation proposed by Fenves and Chopra [7], i.e. analysis type II, are very close for all height ratios and regardless of whether water is considered compressible or not. This observation confirms the effectiveness of the analytical formulation even for dams with a slightly inclined upstream face.

Table 3. Pine Flat dam fundamental mode shapes used.

y/H_s	Normalized mode shape $\psi_1^{(x)}(0, y)/\psi_1^{(x)}(0, H_s)$			
	Fenves and Chopra [19]		Finite element analysis	
	Original mode shape	Cubic interpolation	Original mode shape	Cubic interpolation
1.00	1.000	1.000	1.000	1.000
0.95	0.866	0.866	0.875	0.871
0.90	0.735	0.745	0.752	0.755
0.85	0.619	0.638	0.640	0.650
0.80	0.530	0.544	0.543	0.556
0.75	0.455	0.461	0.461	0.472
0.70	0.389	0.389	0.391	0.398
0.65	0.334	0.327	0.331	0.333
0.60	0.284	0.273	0.279	0.277
0.55	0.240	0.228	0.233	0.228
0.50	0.200	0.189	0.194	0.186
0.45	0.165	0.157	0.159	0.150
0.40	0.135	0.130	0.129	0.120
0.35	0.108	0.108	0.102	0.094
0.30	0.084	0.089	0.080	0.073
0.25	0.065	0.073	0.060	0.056
0.20	0.047	0.058	0.044	0.042
0.15	0.034	0.045	0.030	0.030
0.10	0.021	0.031	0.019	0.019
0.05	0.010	0.016	0.010	0.009
0.00	0.000	0.000	0.000	0.000

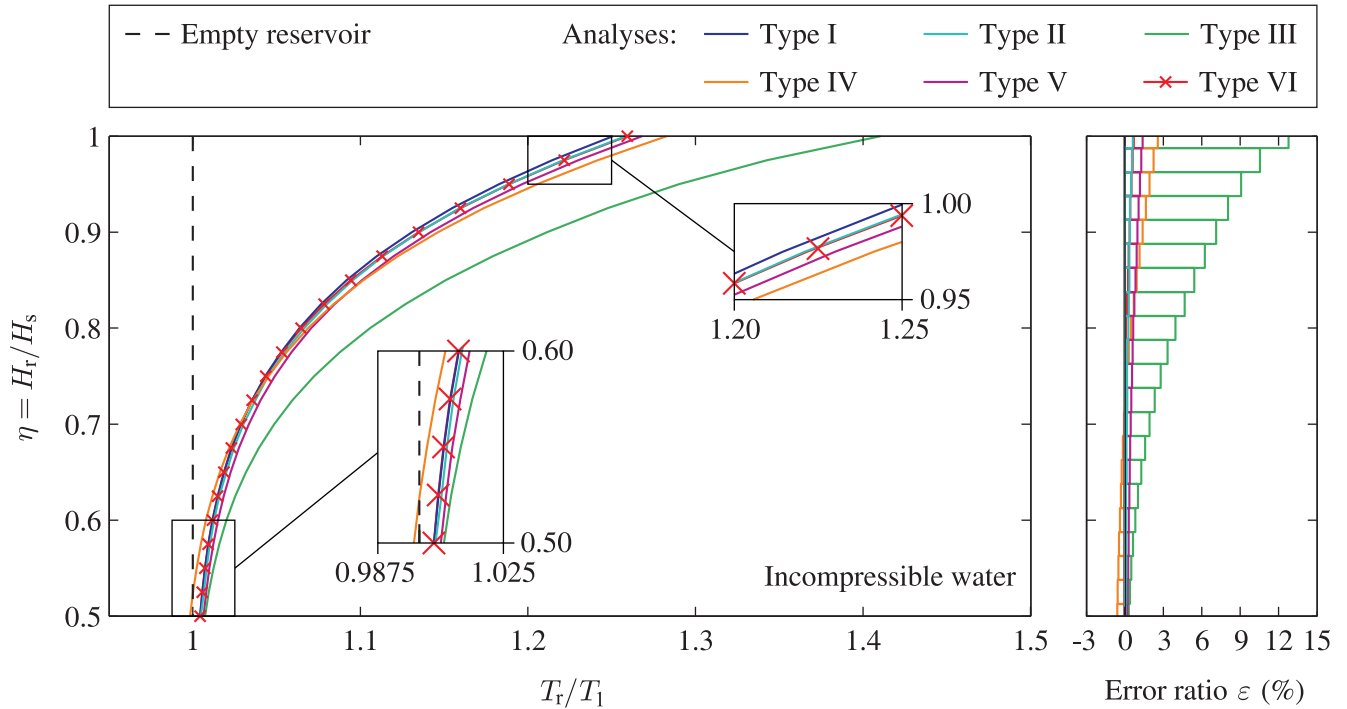


Figure 6. Variation of period ratio T_r/T_1 as a function of reservoir height ratio η assuming incompressible water.

When water compressibility is neglected, Eq. (40) shows that the elasticity modulus of the dam has no effect on the ratio T_r/T_1 , a result that we confirmed numerically and analytically, i.e. using analysis types I and II. Therefore, period ratios T_r/T_1 for incompressible water are illustrated independently of the dam elasticity modulus. Fig. 6 shows that analysis type III using Westergaard added mass predicts the fundamental frequency of the dam-reservoir system with an error of about 12 per cent for a full reservoir in the case of Pine Flat dam. Figs. 6 and 7 also clearly indicate that our simplified procedure, i.e. analysis type VI, yields excellent results regardless of dam stiffness and compressible or incompressible water assumptions. The results of the new simplified procedure remain in very good agreement when approximate parameters are used instead of those obtained from finite element analysis of the dam section, i.e. analysis types IV and V.

To investigate the influence of gravity dam cross-section geometry and dam stiffness on the accuracy of the simplified procedure proposed in this paper, we analyse three typical gravity dam cross-sections with heights varying from 90 m to 35 m as illustrated in Fig. 8. The three dams are denoted D1 to D3 from the highest to the lowest. Finite element models of the dam sections and corresponding dam-reservoir systems are built using the software ADINA [27]. The new simplified method is then applied using approximate parameters, i.e. analysis types IV to V, as well as parameters resulting from finite element analyses of each of the dam sections with an empty reservoir, i.e. analysis type VI. The period ratios T_r/T_1 obtained are illustrated in Fig. 9 considering reservoir height ratios from $\eta = 0.5$ to 1.0 and two moduli of elasticity $E_s = 25$ GPa and $E_s = 35$ GPa. The different analyses are summarized in Table 4 for clarity purposes.

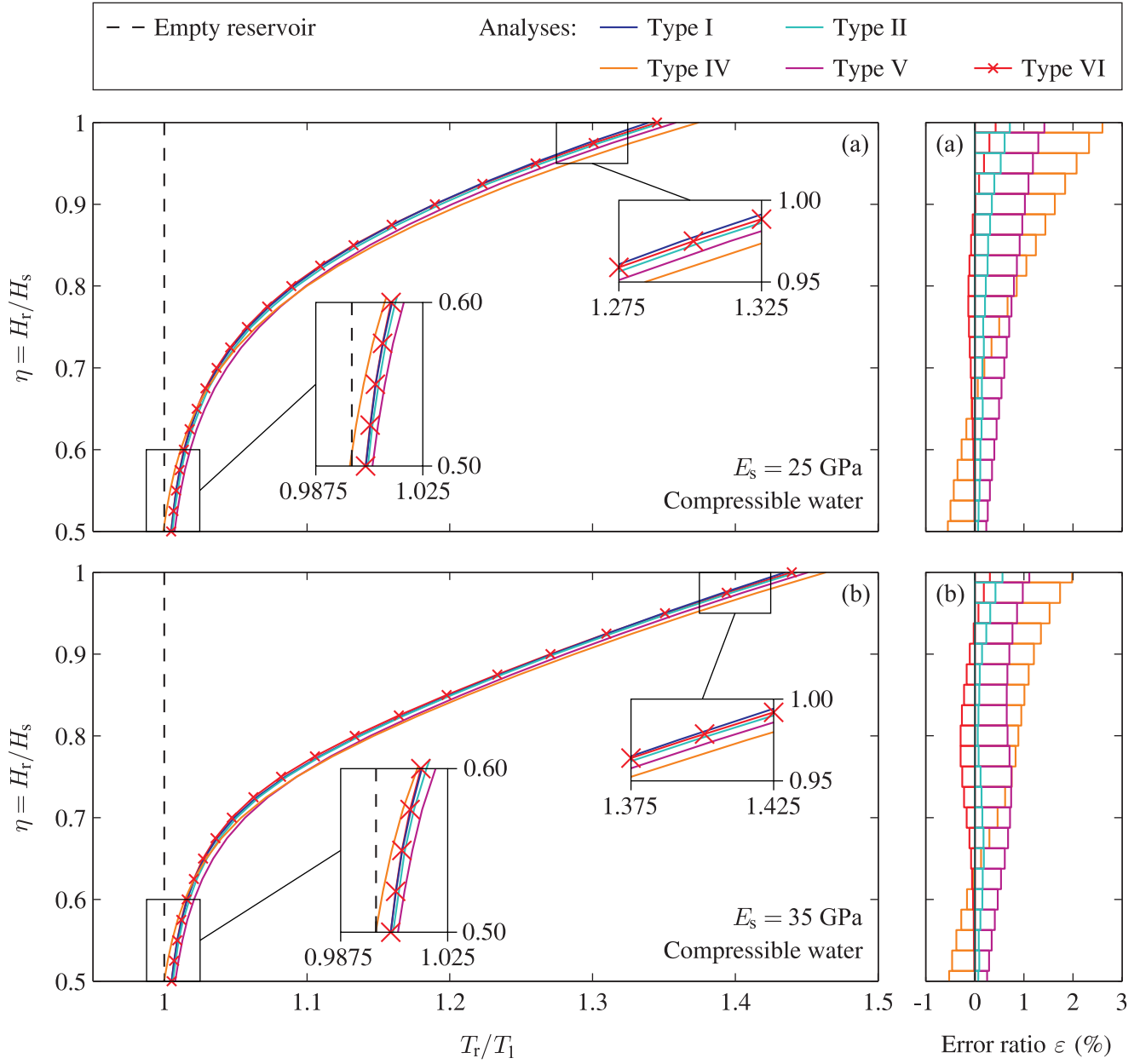


Figure 7. Variation of period ratio T_r/T_1 as a function of reservoir height ratio η considering water compressibility: (a) $E_s = 25$ GPa and (b) $E_s = 35$ GPa.

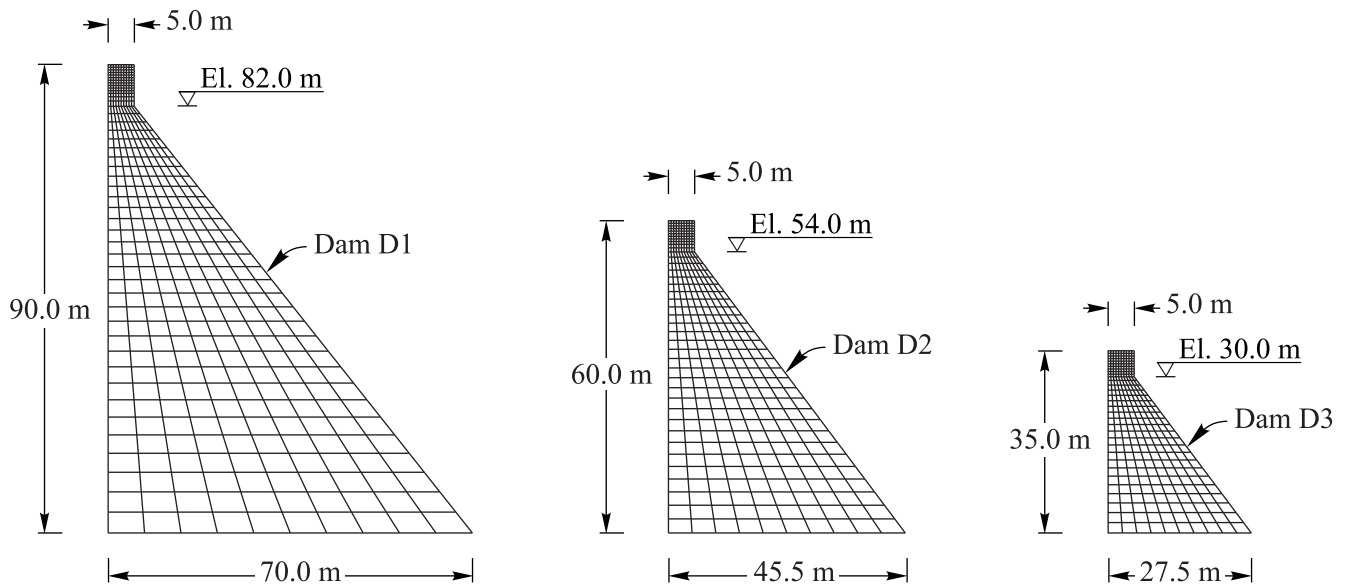


Figure 8. Geometry and finite element models of gravity dam cross-sections D1, D2 and D3.

Table 4. Summary of analysis types conducted.

Water assumption	Analysis	Gravity dam							
		$E_s = 25 \text{ GPa}$				$E_s = 35 \text{ GPa}$			
		Pine Flat	D1	D2	D3	Pine Flat	D1	D2	D3
Incompressible	Type I	x	x	x	x	x	x	x	x
	Type II	x	-	-	-	x	-	-	-
	Type III	x	-	-	-	x	-	-	-
	Type IV	x	x	x	x	x	x	x	x
	Type V	x	x	x	x	x	x	x	x
	Type VI	x	x	x	x	x	x	x	x
Compressible	Type I	x	x	x	x	x	x	x	x
	Type II	x	-	-	-	x	-	-	-
	Type III	-	-	-	-	-	-	-	-
	Type IV	x	x	x	x	x	x	x	x
	Type V	x	x	x	x	x	x	x	x
	Type VI	x	x	x	x	x	x	x	x

We first observe that the results of analysis types I and VI are almost identical for all the studied dam sections independently of water compressibility or incompressibility assumptions, dam geometry and stiffness. Analysis types IV and V yield satisfactory results for the 90-m high dam section D1. They are less accurate however when applied to smaller dam sections D2 and D3. Analysis type IV introduces large discrepancies because it uses approximate fundamental generalized force, generalized mass, mode shape and vibration period that were mainly calibrated using higher standard dam sections [19, 20]. We note that the fundamental period predictions are improved when an input fundamental vibration period obtained from a finite element analysis of the dam with empty reservoir is used instead of Eq. (87), i.e. analysis type V.

Based on the previous findings, we recommend to use the proposed simplified method according to scheme of analysis type VI. The other schemes would provide appropriate results for high gravity dams, while an increasing error is introduced for smaller dams. To assess the accuracy of the proposed method in determining the damping ratio $\tilde{\xi}_1$ of the dam-reservoir system ESDOF, Fig. 10 illustrates the variation of this parameter as a function of reservoir height ratio $\eta \geq 0.5$ considering water compressibility, two moduli of elasticity $E_s = 25$ GPa and $E_s = 35$ GPa and the four gravity dam cross-sections described previously. In this figure, the results determined by applying the proposed method following the scheme of analysis type VI are compared to those obtained using the classical method developed by Fenves and Chopra [7] and reviewed in section 2. The curves clearly show that both techniques yield identical damping ratios for the four dam monoliths.

Finally, denoting $F_{st} = \rho_r g H_r^2 / 2$ the total hydrostatic force exerted on dam upstream face, we determine the normalized equivalent lateral forces $H_s f_1(y) / F_{st}$ considering a unit ordinate of pseudo-acceleration spectrum, water compressibility, a full reservoir, i.e. $\eta = 1$, two moduli of elasticity and the four dams cross-sections as before. Again, the resulting force distributions obtained using the classical and proposed methods are practically coincident for the four dam monoliths studied as illustrated in Fig. 11.

5 Concluding remarks

This paper proposed an original practical method to evaluate the seismic response of gravity dams. We first developed a simplified but yet a rigorous and practical formulation to determine the fundamental period of vibrating dam-reservoir systems and corresponding added damping, force and mass. The new formulation includes the effects of dam geometry and flexibility, water compressibility and varying reservoir level. The mathematical derivations of the method were provided considering both incompressible and compressible water assumptions. In the former case, we proposed a closed-form expression to determine the fundamental vibration period of a dam-reservoir system. When water compressibility is considered, we showed that the fundamental vibration period of a dam-reservoir system can be obtained by simply solving a cubic equation. Simplified expressions to compute the equivalent lateral earthquake forces and the static correction forces are proposed. These forces are to be applied at the dam upstream

face to determine response quantities of interest, such as the stresses throughout the dam cross-section.

To assess the efficiency and accuracy of the proposed technique, several analysis types were applied to dam cross-sections with various geometries and rigidities impounding reservoirs with different levels. The following conclusions could be drawn from the comparison of the period predictions obtained from the different analyses: (i) the analytical formulation of hydrodynamic effects yields accurate predictions when compared to numerical results obtained by modeling the reservoir using potential-based finite elements, (ii) the proposed simplified procedure gives excellent results when the fundamental generalized earthquake force coefficient, generalized mass, mode shape and vibration period are directly obtained from a finite element analysis of the dam with an empty reservoir, and (iii) the fundamental period predictions of the simplified procedure remain satisfactory for large dams while larger discrepancies are observed for smaller ones when approximate parameters are used instead of those obtained from finite element analysis. We also showed that the new procedure yields an excellent estimation of the equivalent damping ratio and equivalent earthquake lateral forces. The proposed technique presents a significant advantage over conventional Westergaard added-mass formulation, namely because it can directly account for dam flexibility and water compressibility, while Westergaard's solution assumes that the dam is rigid and water is incompressible. The analytical expressions developed and the procedure steps were presented in a manner such that calculations could be easily implemented in a spreadsheet or program for practical dynamic analysis of gravity dams. We clearly showed that the proposed procedure can be used effectively for simplified evaluation of the vibration period and seismic response of gravity dams irrespective of their geometry and stiffness.

Acknowledgements

The authors would like to acknowledge the financial support of the Natural Sciences and Engineering Research Council of Canada (NSERC) and the Quebec Fund for Research on Nature and Technology (FQRNT).

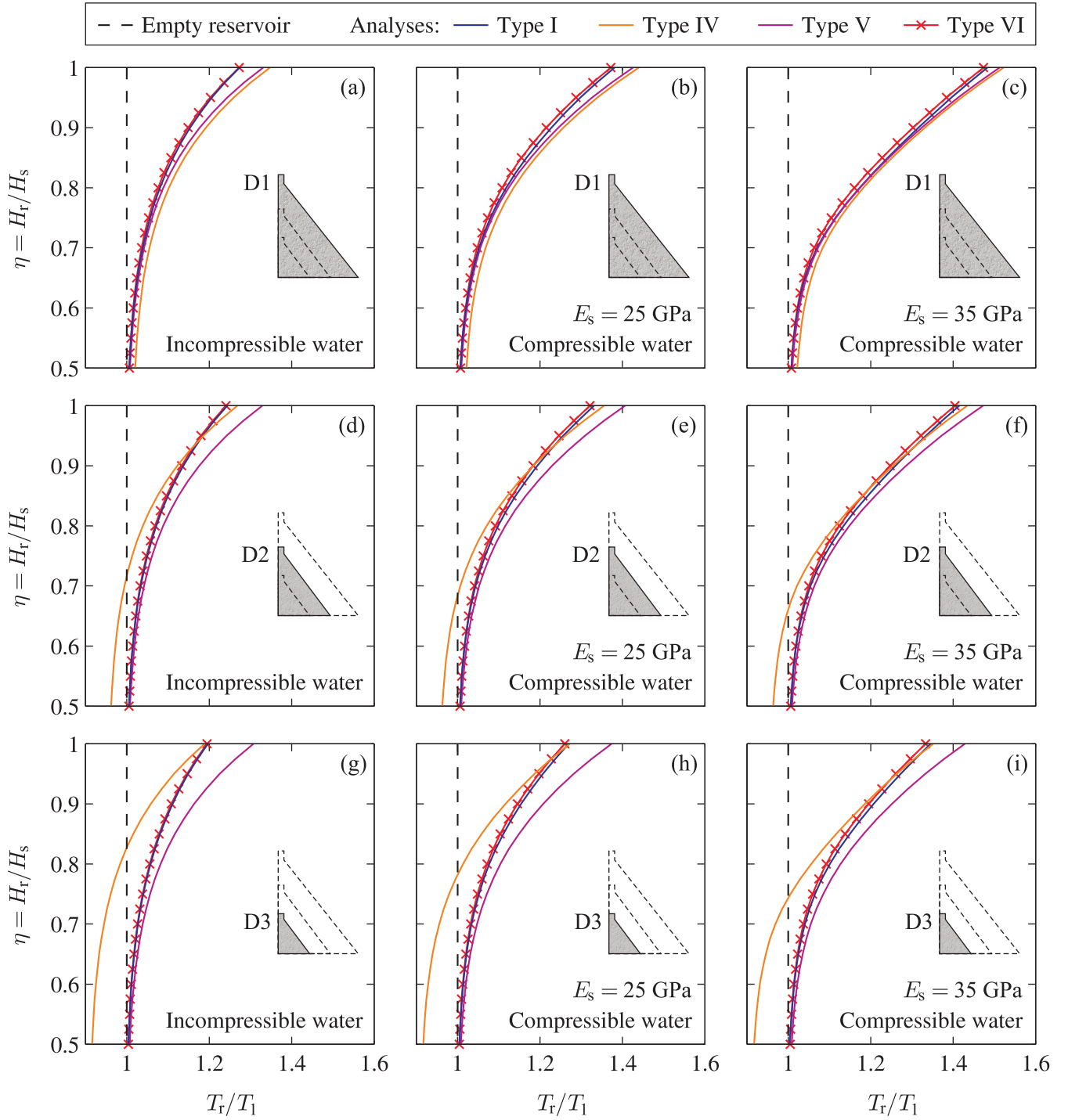


Figure 9. Variation of period ratio T_r/T_1 as a function of reservoir height ratio η considering water compressibility: (a) to (c) Dam D1; (d) to (f) Dam D2; and (g) to (i) Dam D3.

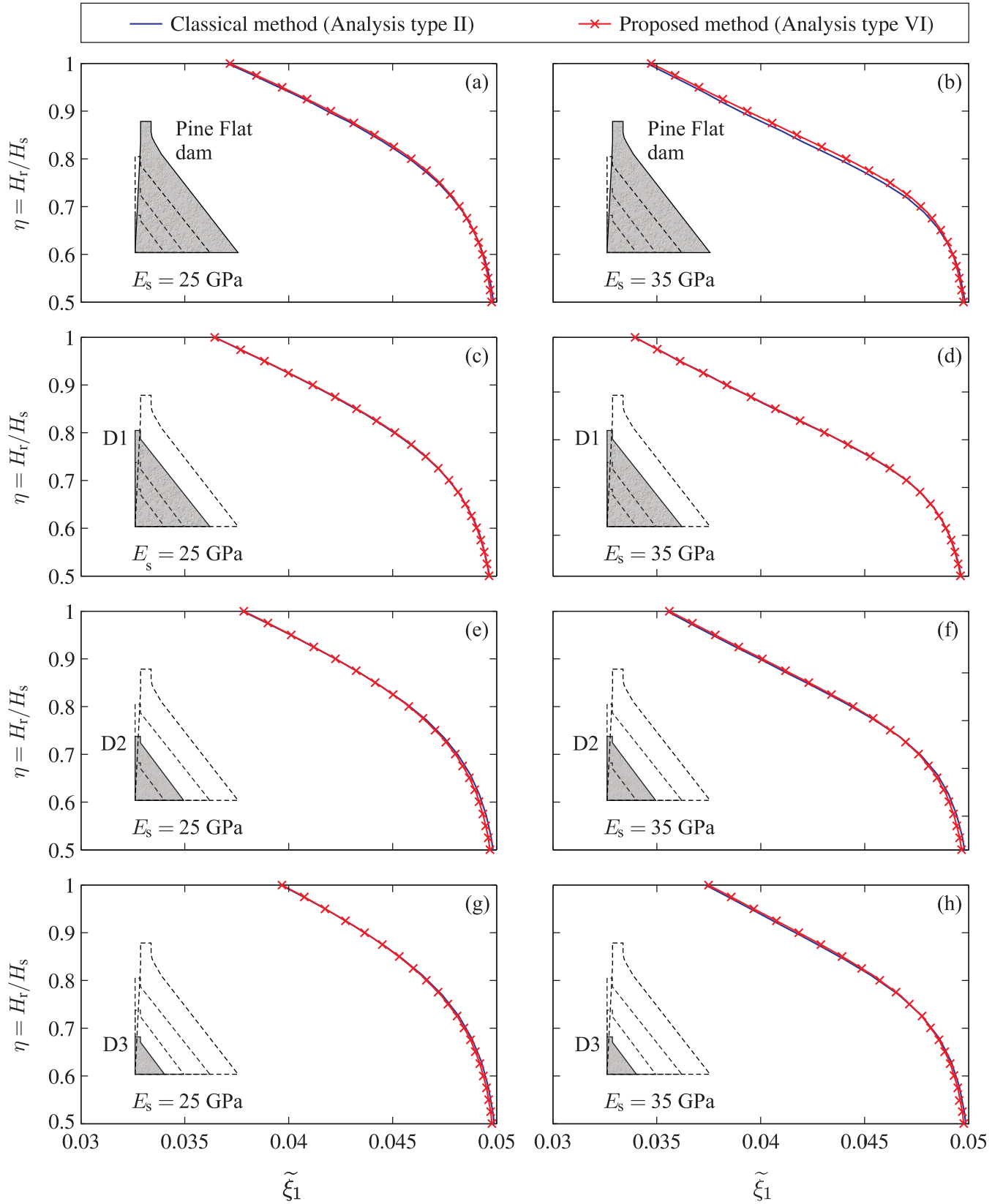


Figure 10. Variation of the damping ratio $\tilde{\xi}_1$ as a function of reservoir height ratio η considering water compressibility: (a) and (b) Pine Flat dam; (c) and (d) Dam D1; (e) and (f) Dam D2; and (g) and (h) Dam D3.

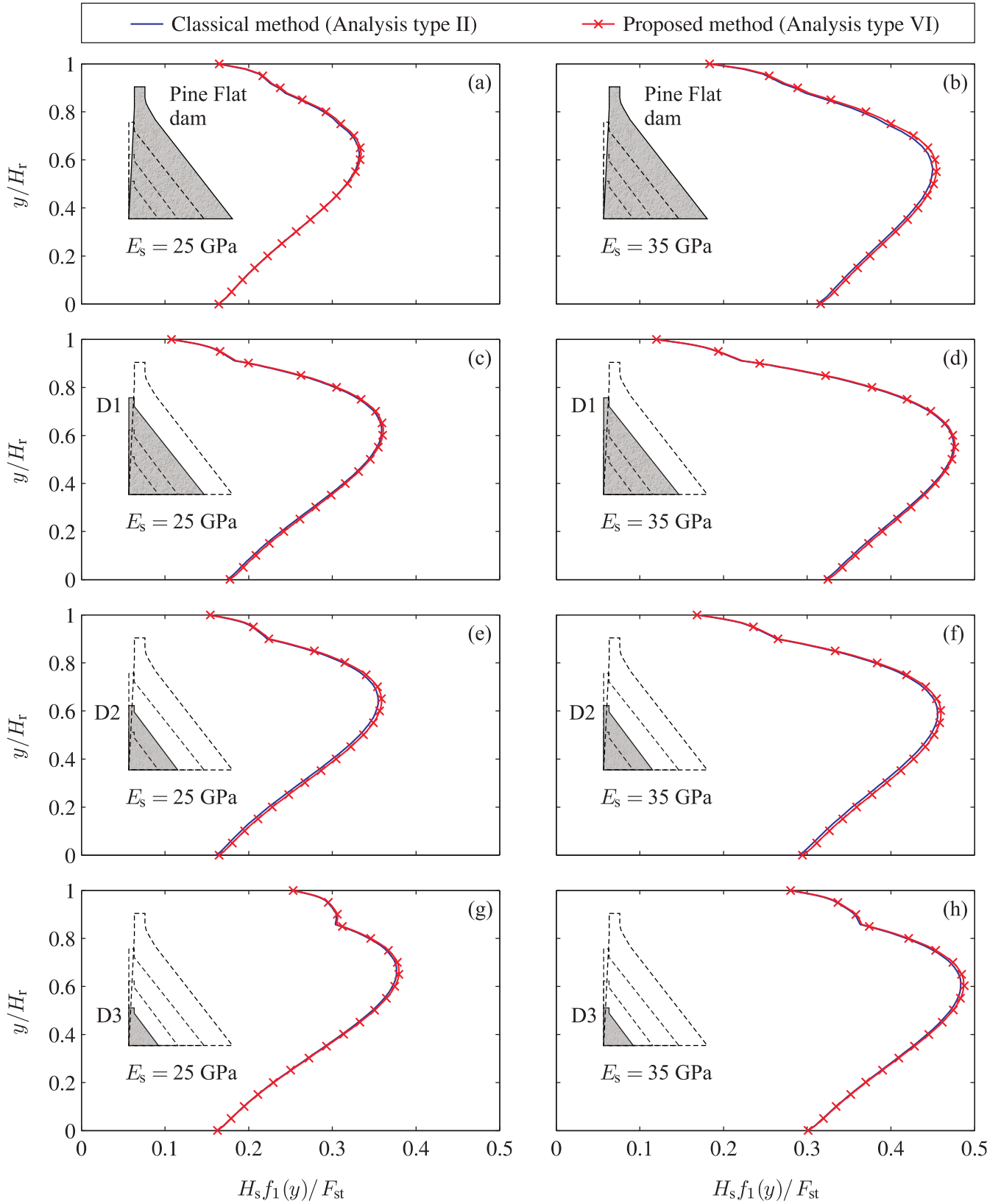


Figure 11. Normalized equivalent lateral earthquake forces corresponding to dam fundamental mode response considering water compressibility: (a) and (b) Pine Flat dam; (c) and (d) Dam D1; (e) and (f) Dam D2; and (g) and (h) Dam D3.

References

- [1] Westergaard HM. Water pressures on dams during earthquakes. *Transactions(ASCE)* 1933; **98**: 418-472.
- [2] Chopra AK. Earthquake response of concrete gravity dams. Report No. UCB/EERC-70/01, University of California, Berkeley, 1970.
- [3] Chakrabarti P, Chopra AK. Earthquake analysis of gravity dams including hydrodynamic interaction. *Earthquake Engineering and Structural Dynamics* 1973; **2**: 143-160.
- [4] Chopra AK. Earthquake resistant design of concrete gravity dams. *Journal of the Structural Division(ASCE)* 1978; **104**: 953-971.
- [5] Saini SS, Bettess P, Zienkiewicz OC. Coupled hydrodynamic response of concrete gravity dams using finite and infinite elements. *Earthquake Engineering and Structural Dynamics* 1978; **6**: 363-374.
- [6] Hall JF, Chopra AK. Two-dimensional dynamic analysis of concrete gravity and embankment dams including hydrodynamic effects. *Earthquake Engineering and Structural Dynamics* 1982; **10**: 305-332.
- [7] G. Fenves, A.K. Chopra, Earthquake analysis and response of concrete gravity dams. Report No. UCB/EERC-84/10, University of California, Berkeley, California, 1984.
- [8] Liu PH, Cheng A. Boundary solutions for fluid-structure interaction. *Journal of Hydraulic Engineering(ASCE)* 1984; **110**(1): 51-64.
- [9] Fok KL, Hall JF, Chopra AK. EACD-3D, a computer program for three-dimensional earthquake analysis of concrete dams. Report No UCB/EERC-86/09, University of California, Berkeley, California, 1986.
- [10] Tsai CS, Lee GC. Arch dam-fluid interactions: by FEM-BEM and substructure concept. *International Journal of Numerical Methods in Engineering* 1987; **24**: 2367-2388.
- [11] Humar JL, Jablonski AM. Boundary element reservoir model for seismic analysis of gravity dams. *Earthquake Engineering and Structural Dynamics* 1988; **16**: 1129-1156.
- [12] Maeso O, Aznarez JJ, Dominguez J. Three-dimensional models of reservoir sediment and effects on the seismic response of arch dams. *Earthquake Engineering and Structural Dynamics* 2004; **33**: 1103-1123.
- [13] Bouaanani N, Miquel B. A new formulation and error analysis for vibrating dam–reservoir systems with upstream transmitting boundary conditions. *Journal of Sound and Vibration* 2010; **329**: 1924-1953.
- [14] Fenves G, Chopra AK. EAGD-84, a computer program for earthquake analysis of concrete gravity dams. Report No UCB/EERC-84/11, University of California, Berkeley, California, 1984.
- [15] Rea D, Liaw CY, Chopra, AK. Dynamic properties of Pine Flat dam. Report UCB/EERC-72/07, University of California, Berkeley, California, 1972.
- [16] Duron Z, Hall J. Experimental and finite element studies of the forced vibration response of Morrow Point Dam. *Earthquake Engineering and Structural Dynamics* 1988; **16**: 1021–1039.
- [17] Proulx J, Paultre P, Rheault J, Robert Y. An experimental investigation of water level effects on the dynamic behaviour of a large arch dam. *Earthquake Engineering and Structural Dynamics* 2001; **30**: 1147-1166.

- [18] Bouaanani N, Paultre P, Proulx J. Two-dimensional modelling of ice-cover effects for the dynamic analysis of concrete gravity dams. *Earthquake Engineering and Structural Dynamics* 2002; **31**: 2083-2102.
- [19] Fenves G, Chopra AK. Simplified analysis for earthquake resistant design of concrete gravity dams. Report No. UCB/EERC-85/10, University of California, Berkeley, 1985.
- [20] Fenves G, Chopra AK. Simplified earthquake analysis of concrete gravity dams. *Journal of Structural Engineering* 1987; **113**(8): 1688-1708.
- [21] Bouaanani N, Paultre P, Proulx J. A closed-form formulation for earthquake-induced hydrodynamic pressure on gravity dams. *Journal of Sound and Vibration* 2003; **261**: 573-582.
- [22] Hatanaka M. Study on the earthquake-resistant design of gravity type dams. *Proceedings of the Second World Conference on Earthquake Engineering*, Tokyo and Kyoto, Japan, 1960; **II**: 82.1–82.16.
- [23] Okamoto S. *Introduction to earthquake engineering*. 2nd edition, University of Tokyo Press: Tokyo, 1984.
- [24] Bouaanani N, Lu FY. Assessment of potential-based fluid finite elements for seismic analysis of dam–reservoir systems. *Journal of Computers and Structures* 2009; **87**: 206-224.
- [25] Reinhardt F, Soeder H. *dtv-Atlas zur Mathematik*. Deutscher Taschenbuch Verlag: Munich, 2001.
- [26] Clough RW, Penzien J. *Dynamics of Structures*, McGraw-Hill, Inc., New York, 1975.
- [27] ADINA Theory and Modeling Guide. Report ARD 06-7. ADINA R & D, Inc., 2006.